BTO 2016.015 | May 2016

BTO report

Iron and manganese removal: recent advances in modelling of the treatment efficiency by rapid sand filtration

KWR Watercycle Research Institute

BTO

Iron and manganese removal: recent advances in modelling of the treatment efficiency by rapid sand filtration

BTO 2016.015 | February 2016

Project number
400554-029

Project manager
Erwin Beerendonk

Client
BTO - Thematic research - Water and energy

Quality Assurance
dr. ir. E.C. (Emile) Cornelissen

Author(s)
dr. ir. D. (Dirk) Vries, dr. ir. C. (Cheryl) Bertelkamp

Sent to
BTO TG DTT

Year of publishing
2016

More information
dr.ir. Dirk Vries
T 671
E dirk.vries@kwrwater.nl

Keywords

PO Box 1072
3430 BB Nieuwegein
The Netherlands

T +31 (0)30 60 69 511
F +31 (0)30 60 61 165
E info@kwrwater.nl
I www.kwrwater.nl

KWR Watercycle Research Institute

BTO *Managementsamenvatting*

Nieuw procesmodel geeft zicht op prestatie snelle zandfilters in verwijdering van ijzer, mangaan en ammonium

Auteur(s) dr.ir. Dirk Vries en dr.ir. Cheryl Bertelkamp

Een nieuw ontwikkeld procesmodel blijkt goed in staat om onder verschillende condities (bijvoorbeeld zuurgraad en contacttijd) te voorspellen in hoeverre ijzer en mangaan uit grondwater worden verwijderd over de hoogte van het filterbed en in het uitgaande water. De resultaten bieden een solide basis voor doorontwikkeling van het model voor complexere filtratieprocessen waarin interactie met ammonium, korte- (door spoeling) en lange termijneffecten (aangroei van ijzer- en mangaanafzettingen) en filtratie met verschillende filtermateriaallagen een belangrijke rol spelen. We geven een overzicht van modelvormend werk naar de verwijderingsprestaties van snelle zandfilters en verdiepen het inzicht in oxidatief-adsorptieve processen en in de biologische verwijdering van ammonium. De combinatie van snelle zandfiltratie en beluchting is een veel toegepaste methode voor de verwijdering van ammonium, ijzer en/of mangaan uit (grond)water op drinkwaterproductielocaties in Nederland.

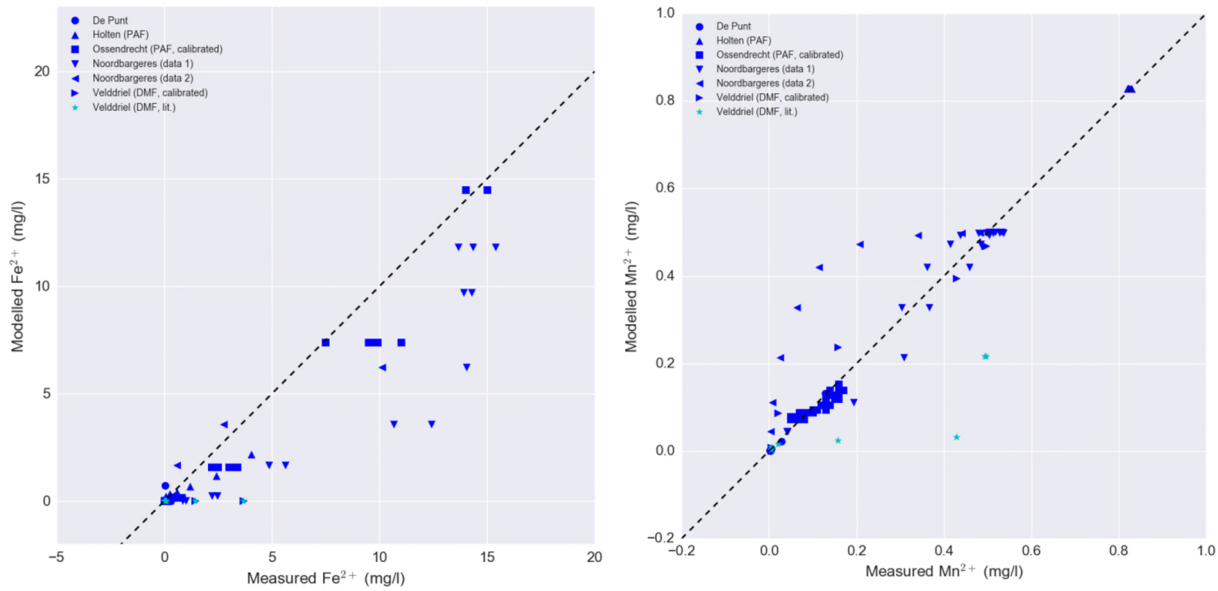

Vergelijking van modelresultaten (verticaal) en meetwaarden (horizontaal)) voor een aantal Nederlandse grondwaterzuiveringslocaties. Links: ijzer(II)-concentraties, rechts: mangaan(II)-concentraties.

Belang: onderbouwing snelfiltratie als veel toegepaste methode voor metaalverwijdering

In grondwater kunnen de tweewaardige ionen ijzer (0,01 – 20 mg/L) en mangaan (0,001 – 1 mg/L) aanwezig zijn. Snelfiltratie is een veel toegepaste methode om deze metalen via oxidatie en adsorptie te verwijderen en ter stimulatie van het biologische nitrificatieproces dat ammonium uit het water haalt. Ondanks het veelvuldige gebruik van snelfilters is de kennis hierover echter erg versnipperd: hoe de filters worden gespoeld en hoe hoog de bovenwaterstand en de bedhoogte moeten zijn, wordt bijvoorbeeld vaak ad hoc bepaald. Met het ontwikkelde model willen we hierin verandering brengen. Enerzijds gebeurt dit door het vastleggen van kennis, anderzijds moet het model

procestechnologen en onderzoekers helpen in hun evaluatie van huidige filters of ontwerp van nieuwe snelfilters. . Door variatie in verschillende condities maakt een gevalideerd model de analyse en optimalisatie van een bedrijfsproces mogelijk, zonder dit te verstoren.

Aanpak: modelvorming en ondersteuning door experimenten

Het ontwikkelde model beschrijft de mechanismen waarmee een snelfilter de metalen ijzer en mangaan verwijdert: met oxidatie na beluchting in het ingaande water, en met adsorptie en oxidatie van de metaalionen aan het filtermateriaal. De adsorptieve-oxiderende stap hangt sterk af van de zuurgraad van het water en van het ontwikkelde laagje ijzer- en mangaanoxiden op het filtermateriaal. Aan de hand van een literatuurstudie en adsorptieproeven is in kaart gebracht hoe het adsorberend vermogen van filtermateriaal verschilt voor een aantal Nederlandse grondwaterzuiveringslocaties en contacttijd (gemeten middels variatie in de bedhoogte). Op grond hiervan is de verwijderingsefficiëntie van de afzonderlijke snelfilters doorgerekend.

Resultaten: adsorptie varieert sterk per locatie en over de bedhoogte van het filter

Uit één productielocatie is filtermateriaal op verschillende dieptes bemonsterd nadat deze enkele maanden ervoor was ingebracht. Vervolgens is de adsorptiecapaciteit vastgesteld. Uit experimentele bepalingen en berekeningen blijkt dat adsorptie bovenin het filterbed begint, en dat de mate van adsorptie sterk afhangt van het filtermateriaal. Ook tonen de simulaties aan dat een juiste inschatting van modelparameters voor adsorptie, maar ook voor oxidatie in het filter, cruciaal zijn voor een juiste voorspelling. Daarnaast kan de variatie in adsorptie tussen productielocaties sterk verschillen. Tot slot blijkt op grond van het onderzoek dat bij afnemende zuurgraad (hogere pH) van het grondwater, de adsorptiecapaciteit van het filtermateriaal toeneemt.

Implementatie: doorontwikkeling naar gebruiksvriendelijk analysetool metaalverwijdering

Het ontwikkelde procesmodel, met daarin de vastgelegde kennis over snelfiltratie, biedt een solide basis voor het beschrijven van complexere of alternatieve verwijderingsmechanismen, zoals de verwijdering van arseen. In vervolgonderzoek wordt het model doorontwikkeld naar een gebruiksvriendelijke analysetool. Hiermee kunnen gebruikers (waterbedrijven, onderzoekers) de effecten van conditionering van water en alternatieve procescondities bestuderen, zonder bedrijfsprocessen te verstoren.

Rapport

Dit onderzoek is beschreven in:

- Het rapport *Iron and manganese removal: recent advances in modelling treatment efficiency by rapid sand filtration* (BTO 2016.015).
- Manuscript ingediend bij *Water Research*: *Iron and manganese removal: recent advances in modelling treatment efficiency by rapid sand filtration*. Gereviseerde versie ingediend d.d. 01-11-2016 (na schrijven dit rapport).

More information
dr.ir. Dirk Vries
T 671
E dirk.vries@kwrwater.nl

KWR
PO Box 1072
3430 BB Nieuwegein
The Netherlands

KWR Watercycle Research Institute

Voorwoord

De voorliggende studie bevat een beknopt overzicht van de behaalde resultaten in het modelvormende onderzoek naar snelfiltratie bij grondwaterzuivering. Het is in een manuscript voor een wetenschappelijk tijdschrift gegoten en vormt de ruggengraat van dit rapport. Het onderzoekswerk is dankzij BTO-gelden én extra financiële middelen door speerpuntgelden van Vitens (en in het verleden door Oasen) gefinancierd.

Snelfiltratie wordt al decennia door waterbedrijven zeer veel toegepast in de zuivering, en niet alleen bij grondwaterzuivering. Dit proces is van belang voor de verwijdering van ijzer en mangaan, maar ook van ammonium. Toen de eerste onderzoeken rondom een snelfiltratiemodel in 2010 waren gestart, was de hoop en de verwachting dat een model in afzienbare tijd kon worden ontwikkeld. De ingrediënten waren er: een speciatieprogramma PHREEQC die zich reeds in de ondergrond (geochemie) had bewezen als een adequaat modelleerinstrument voor chemie (speciatie) en (eenvoudig) transport, ervaringen en kennis in de bedrijfstak, het nagenoeg parallel lopende onderzoek van Jantinus Bruins (WLN, UNESCO-IHE), het model in STIMELA (TU Delft) en een frisse kijk. Het bleek toch een lastige kluif. Nu, enkele speerpuntprojecten en collectieve projecttijd verder, kunnen we eindelijk spreken van een model die tenminste de werkelijkheid van enkele filters kan nabootsen. Helaas kunnen we nog steeds niet met zekerheid vaststellen of het model niet teveel vrijheidsgraden heeft (of met andere woorden, enkele modelparameters te grote variatie vertonen bij verschillende snelfilters). Daarvoor is meer data uit de praktijk nodig, en is een hechtere samenwerking met de waterbedrijven noodzakelijk. Deze ambitie zal worden gerealiseerd in een vervolgproject 'IJzersterke tool', waarbij het doel is om het model voor ontijzering en ontmanganing in een softwaretool te schrijven ten behoeve van verdere validatie, analyse en optimalisatie.

We willen tenslotte alle collega's van waterbedrijven hartelijk bedanken voor hun inzet en geloof in de meerwaarde van het kwantitatief beschrijven van de interessante processen en mechanismen die zich bij deze zuiveringsstap voordoen:

Frank Schoonenberg (Vitens)
Weren de Vet (WML)
Jantinus Bruins (WLN)
Jos Dusseldorp (Oasen)
Simon Dost (WMD)
Jan Bahlman (Evides)
Patrick Teunissen (Vitens),
Gerrit-Jan Zweere (Vitens),

plus de leden van de themagroep Drinkwatertechnologie van de Toekomst.

En last but not least, de collega's en oud-collega's die tijdens het onderzoek hun steentje hebben bijgedragen: Benjamin van den Akker, Bas Hofs, Bas Wols, Maarten Nederlof, Erwin Beerendonk en Emile Cornellissen.

Beknopte samenvatting (abstract)

Een model is ontwikkeld die rekening houdt met de belangrijke karakteristieken van (natte) snelfiltratie: de waterkwaliteitsparameters alkaliniteit, pH en temperatuur van het ingaande water, de (homogene) oxidatiekinetiek in de bovenwaterlaag, binding van ijzer(II) en mangaan(II) aan de oppervlakte van het filtermateriaal en sequentiële (heterogene) oxidatie en tenslotte de procescondities: enkellaags- of dubbellaagsfiltratie, verblijftijd, hoogte van het filterbed en filtratiesnelheid. Aannames zijn gemaakt om validatie van het model met praktijkdata zo eenvoudig mogelijk te maken, zonder in te hoeven boeten op de belangrijkste verwijderingsmechanismen. Van verscheidene grondwaterproductielocaties zijn adsorptie-isothermen bepaald. Deze isothermen tonen dat adsorptie van ijzer(II) en mangaan(II) substantieel varieert tussen locaties, en dat adsorptie toeneemt met verhoogde pH (van het influent-water). Het model blijkt verder gevoelig voor (experimenteel) bepaalde adsorptieparameters, de heterogene oxidatiesnelheidsconstante en de filtratietijd. Model resultaten komen goed overeen met de metingen indien de adsorptie-isotherm van het filtermateriaal bekend is en de heterogene oxidatieconstante gekalibreerd.

Contents

1 Introductie

1.1 Aanleiding en achtergrond

Grondwater kan concentraties van enkele tienden milligram per liter tot wel 20 milligram per liter aan (tweewaardig) ijzer en enkele tienden microgram tot wel een milligram per liter mangaan (ook een tweewaardig ion). Naast ijzer(II) en mangaan(II) kan er ook ammonium aanwezig zijn in grondwater. Een effectief verwijderingsproces is van belang, omdat bij ineffectieve ijzer- of mangaanverwijdering ongewenste effecten kunnen optreden, zoals bruinwaterklachten, metaalsmaak, afzetting van ijzer- en mangaanprecipitaten in het leidingnet en verhoogde biofilmvorming door hechting van micro-organismen aan deze precipitaten. Snelfiltratie is een veel toegepaste methode om via oxidatie en adsorptie deze metalen te verwijderen en het biologische nitrificatieproces te stimuleren ten behoeve van ammoniumverwijdering. Deze mechanismen worden in paragraaf 0 en 2.2 verder uitgediept.

Via praktijkervaring en proefonderzoek worden snelfilters opgestart en bedreven, echter, de operationele kennis is versnipperd en toegepaste strategieën voor het spoelen van filters, de hoogte van de bovenwaterstand en de gehanteerde bedhoogte zijn vaak ad hoc ingesteld. Bij (drink)waterbedrijven is daarom de behoefte ontstaan om wetenschappelijke literatuur en praktijkkennis te inventariseren en de verschillende mechanismen die tijdens verschillende operationele fases van snelfiltratie actief zijn, vast te leggen in een model. Uit eerder BTO-onderzoek (Kennisinventarisatie ontijzering [5]), (Kennisinventarisatie ontmanganing [9]) en speerpuntonderzoek voor Vitens ([7], [8]) zijn kennisleemtes geïnventariseerd en is aan modelvorming voor ontijzering en ontmanganing gewerkt. De modellen die ontwikkeld zijn voor de verwijdering van mangaan en ijzer, voorspellen aan de hand van de gegeven situatie (waterkwaliteit influent, procesontwerp) de ijzer- en mangaanverwijdering slechts ten dele. Homogene[1] ijzerverwijdering onder beluchte condities bij natfiltratie is uitgezocht en in een model uitgewerkt [8]. De rol van biologisch gevormd mangaanhoudend mineraal dat de ontmanganing versnelt, wordt in een promotie-onderzoek aan UNESCO-IHE bestudeerd. Voor andere verwijderingsmechanismen zijn er 'conceptmodellen' ontwikkeld, onder andere voor ontmanganing, heterogene[2] (adsorptieve) ontijzering en heterogene (biologische) ontijzering. Effecten van de ruwwaterkwaliteit zijn meegenomen, met uitzondering van methaan en ammonium.

In de bedrijfstak ontstond de wens om met het te ontwikkelen en valideren model, de verschillende onderwerpen vast te leggen, maar ook om te dienen als basis voor simulatiegereedschap ten behoeve van analyse door procestechnologen bij waterbedrijven en onderzoekers. Met een gevalideerd model kunnen verschillende condities, zoals zuurgraad van het ingaande water, ijzer- en mangaanbelasting, bovenwaterstand en bedhoogte gevarieerd worden ten behoeve van analyse en optimalisatie van procescondities (zoals conditionering, vaker of minder vaak spoelen, …), zonder het bedrijfsproces te verstoren.

[1] Met homogene ontijzering wordt de omzetting van ijzer(II)-ionen door oxidatieve processen bedoeld.
[2] Met heterogene ontijzering wordt de autokatalytische omzetting van ijzer(II)-ionen door een combinatie van adsorptieve en oxidatieve processen bedoeld.

Met deze stip op de horizon is het BTO-onderzoek '*De onderste korrel boven: : relaties tussen waterkwaliteit, fysisch-chemische omgevingsfactoren en de effectiviteit van ontijzering, ontmanganing en nitrificatie in de zuivering ontrafeld'* gestart.

1.2 Project: de onderste korrel boven

Het beschrijven van de verwijdering van stoffen in snelfiltratie, specifiek ijzer(II), mangaan(II) en ammonium is complex, gezien de afhankelijkheden tussen de verschillende verwijderingsprocessen en het feit dat veel factoren die een rol spelen: de ingaande waterkwaliteit, bijdrage van biologische ijzer- of mangaanverwijdering en fysisch/chemische aspecten die beïnvloed worden door bedrijfsvoering en filtermateriaal. Deze kunnen niet los van elkaar worden gezien en bovendien laten meetcampagnes op bedrijfsinstallaties een beperkt testbereik[3] toe.

1.2.1 Doelstellingen

Het projectplan van 'de onderste korrel boven' formuleert daarom de volgende doelstellingen om de complexiteit te beschrijven en te begrijpen:

1. een beter begrip van ontijzering en ontmanganing door bundeling en verdieping van reeds bestaande kennis;
2. een gevalideerd model dat inzetbaar is voor modelgebaseerde procesvoering bij uiteenlopende typen ruwwater en condities bij snelfiltratie; en tenslotte
3. integratie van de meest recente kennis in het model.

Enkele van de doelstellingen zijn, vaak deels, in samenhang met speerpuntprojecten in opdracht van Vitens gedurende de periode 2013-2015 gerealiseerd. Voortgang en kennis uit die speerpuntprojecten is, in overleg met een begeleidingsgroep met daarin vertegenwoordigers van waterleidingbedrijven (Frank Schoonenberg, Weren de Vet, Jos Dusseldorp, Jantinus Bruins, Simon Dost), zoveel als mogelijk ingezet.

1.2.2 Activiteiten en aanpak

Om de doelstellingen te realiseren is een aanpak gekozen waarbij modelvorming is ondersteund door literatuur- en experimenteel onderzoek. In het projectplan zijn de volgende activiteiten geformuleerd:

1. *Casus doorslag van ijzerhoudende deeltjes (2014)*
   Bij een productielocatie van Vitens (2014), namelijk WPB Culemborg, wordt doorslag van ijzerhoudende deeltjes geconstateerd. De casus biedt een eerste aanzet voor modellering van gevormde ijzerdeeltjes, ondersteund door metingen met onder andere deeltjestellers van in en uitgaand water bij reguliere operationele instellingen (deze zijn niet gevarieerd).
2. *Organisatie van een workshop (2014)*
   Resultaten uit het lopende onderzoek worden gepresenteerd tijdens een workshop te . De workshop geeft een breed overzicht van lopend, toegepast onderzoek op het gebied van processen die in snelfilters plaatsvinden, bedrijfservaringen en modellering van snelfilters en tenslotte innovatieve meetmethoden (qPCR, en echografie toegepast op het filterbed).
3. *Begeleidingsgroepen (2014-2015)*
   De ontwikkelingen en validatie van het model worden afgestemd met een

[3] Zowel variatie in waterkwaliteit, als ook die van fysische parameters (temperatuur, pH) en bedrijfsvoeringparameters is variatie slechts in zeer geringe mate mogelijk.

begeleidingsgroep. Daarnaast vindt er kennisdeling plaats met speerpuntonderzoek op het gebied van snelfiltratie en ijzer- en mangaanverwijdering (opdrachtgever Vitens) en door deelname van KWR aan de begeleidingsgroep van Jantinus Bruins (WLN) in het kader van zijn onderzoek naar mangaanverwijdering, en de begeleidingsgroep van Frank Schoonenberg (Vitens) in het kader van zijn onderzoek bij Vitens naar ijzerverwijdering.

4. *Verdere modelvorming en validatie (2014-2015).*
   Dit werkpakket van activiteiten bestaat uit deelonderzoeken, waar gedurende 2014 een prioritering in is aangebracht. De prioritering is gecursiveerd:
   a. *Het model voor verwijdering van ijzer en mangaan wordt getoetst aan de hand van een set aan metingen en praktijkdata bij verschillende locaties.* Zie Hoofdstuk 2.
   b. *Parameters voor adsorptie van ijzer en mangaan aan praktijkmateriaal* uit voor- en na-filters worden op basis van flesexperimenten onderzocht (zie Hoofdstuk 2) en in het model opgenomen.
   c. Modellering van biologische ijzerverwijdering op basis van datasets van Oasen en WMD en/of Pidpa, en *ammoniumverwijdering door nitrificatie* en denitrificatie.
   d. Beschrijving van de effecten van methaan en gasophoping in het filter, en het voorkomen van gerelateerde problematiek in de filterwerking.
5. *Casus proefinstallatie-onderzoek (no-go in 2015)*
   Het idee is om modelondersteuning en –verbetering te bieden die ondersteund zou worden door proefinstallatieonderzoek bij WMD. Dit onderzoek is in 2015 met onbepaalde tijd uitgesteld.
6. *Implementatie model (2015)*
   Het ontwikkelde model is getoetst met data uit de volgende productielocaties: Holten (Vitens), Velddriel (Vitens), De Punt (Waterbedrijf Groningen), Noordbargeres (Waterbedrijf Groningen), Ossendrecht (Evides).
7. *Disseminatie en rapportage (2015)*
   Het model en de modelresultaten worden vastgelegd in een rapport en (congres)publicatie, zie Hoofdstuk 2.

Gedurende het project zijn, in overleg met de begeleidingsgroep, ambities voor het uitvoeren van activiteiten uit het projectplan op de volgende punten bijgesteld:

- Activiteit (**1**) is beperkt tot experimentele ondersteuning waarvan een notitie is uitgebracht. Er is wel aan een *work-around* gewerkt om deeltjesdoorslag toe te laten in het model.
- Activiteiten (**5**: proefinstallatie-onderzoek) en (**6**: implementatie model) zijn komen te vervallen, ook omdat daartoe geen geschikte locatie en middelen gevonden kon worden. Daarvoor in de plaats is de focus verlegd naar verdieping van activiteit (**3**: modeltoetsing en -validatie) en (**7**: kennisdisseminatie).
- Rapportage in activiteit (**7**) is gecombineerd met het indienen van een manuscript ter publicatie in een wetenschappelijk tijdschrift (zie hoofdstuk 2). Dat heeft geleid tot voorliggend rapport, waarbij de conclusies zijn ingesloten in het manuscript en de managementsamenvatting. Resultaten die niet in de scope van het manuscript passen zijn elders opgenomen: d.w.z. de implementatie en toetsing van het nitrificatiemodel (bijlage II), variatie van de dispersiecoëfficiënt en filtratiesnelheid (speerpuntonderzoeksrapport BTO 2016.042).

1.3 Leeswijzer

In de leeswijzer zijn de gerapporteerde opbrengsten per activiteit geordend, met uitzondering van activiteiten (3: begeleidingsgroepoverleg), (5: proefinstallatie-onderzoek), (6: modelimplementatie) en (7: rapportage, zie activiteit 4).

TABEL 1: LEESWIJZER VAN DIT RAPPORT

Activiteit	Beschrijving	Dit rapport	Anders
1	Doorslag van ijzerhoudende deeltjes	n.v.t.	Notitie
2	Organisatie van een workshop	n.v.t.	Workshop 3/4/2015
4	Modelvorming en validatie a) Toetsing met experimenten en data afkomstig van productielocaties b) Parameters voor adsorptie c) Ammoniumverwijdering door nitrificatie	Hoofdstuk 2, methode (a—c): par. 2.2; resultaten: par. 2.4 en bijlage III, (a): par. 2.4.3; (b) par. 2.4.2.2 (c): bijlage II. Conclusies: par. 2.5.	n.v.t.

1.4 Referenties

[1] W.W.J.M. de Vet. Biological drinking water treatment of anaerobic groundwater in trickling filters, PhD thesis, Delft University of Technology, 2011.

[2] S.K. Sharma, Adsorptive iron removal from groundwater, PhD Thesis, Wageningen University, 2001.

[3] R. Buamah, B. Petrusevski and J. C. Schippers. Oxidation of adsorbed ferrous iron: kinetics and influence of process conditions; Water Science & Technology, 2009, vol 60(9), pp 2353–2363.

[4] D. van Halem, S. G. J. Heijman, R. Johnston, I. M. Huq, S. K. Ghosh, J. Q. J. C. Verberk, G. L. Amy and J. C. van Dijk. Subsurface iron and arsenic removal: low-cost technology for community-based water supply in Bangladesh, Water Science and Technology 62(11), 2010, pp 2702 – 2709.

[5] B. Hofs, Kennisinventarisatie ontijzering, Rapport BTO 2011.018, 2011.

[6] K. Teunissen, A. Abrahamse, H. Leijssen en H. van Dijk. De wondere wereld van deeltjes in het pompstation, H2O vol 40(13), 2007, pp 41—44.

[7] D. Vries, B.A. Wols, B. Hofs. Iron removal in rapid sand filtration: preliminary modelling results; A case study of WTP Holk (Vitens) and WTP Lekkerkerk (Oasen). BTO 2013.204(s).

[8] D. Vries, B. van den Akker. Iron removal in rapid sand filtration: modelling results. Sensitivity analysis and a case study of heterogeneous iron removal at WTP Holten. BTO 2013.207(s).

[9] R. Hofman-Caris, B. Hofs, D. Vries, J. Bruins. Kennisinventarisatie ontmanganing. BTO 2013.018.

2 Manuscript of scientific paper

Iron and manganese removal: recent advances in modelling treatment efficiency by rapid sand filtration

Authors: D. Vries[a], C. Bertelkamp[a], F. Schoonenberg Kegel[b], B. Hofs[c], J. Dusseldorp, J. Bruins, W. de Vet[e], B. van den Akker

Affiliations:

[a]KWR Watercycle Research Institute, P.O. Box 1072, 3430 BB, Nieuwegein

[a]Vitens N.V., P.O. Box 1205, 8001 BE Zwolle, The Netherlands

[c] Evides Waterbedrijf, P.O. Box 4472, 3006 AL Rotterdam, The Netherlands

[d] Waterlaboratorium Noord, Rijksstraatweg 85, 9756 AD, Glimmen, The Netherlands

[e] Water Supply Company Limburg (WML), Limburglaan 25, 6229 GA Maastricht, Netherlands

Abstract. A model has been developed that takes into account the main characteristics of (submerged) rapid filtration: the water quality parameters of the influent water, notably pH, iron(II) and manganese(II) concentrations, homogeneous oxidation in the supernatant layer, surface sorption and heterogeneous oxidation kinetics in the filter, and filter media adsorption characteristics. Simplifying assumptions are made to enable validation in practice, while maintaining the main mechanisms involved in iron(II) and manganese(II) removal. Adsorption isotherm data collected from different Dutch treatment sites show that Fe(II)/Mn(II) adsorption may vary substantially between them, but generally increases with higher pH. The model is sensitive to (experimentally) determined adsorption parameters and the heterogeneous oxidation rate. Model results coincide with experimental values when the heterogeneous rate constants are calibrated.

2.1 Introduction

The main (60%) source for drinking water production in The Netherlands is groundwater. Abstracted groundwater is generally anaerobic and thus requires aeration followed by rapid sand filters to remove iron(II) and manganese (II). Iron and manganese need to be removed from the water, since their presence in water can result in: (1) the sedimentation of iron/manganese precipitates in distribution pipelines which can cause clogging potentially leading to increased energy loss, (2) iron/manganese precipitates in the distribution pipelines can re-suspend during temporary higher discharges leading to discoloured water at the customer tap, (3) metallic taste and odour and (4) staining of laundry and household fixtures (Carlson et al., 1997; Buamah, Petrusevski, Ridder, et al., 2009; Jez-Walkowiak et al., 2015).

According to the Directive 98/83/EC and the Dutch Directive (Drinkwaterbesluit) the maximum concentration levels in drinking water should not exceed 0.20 mg/L for iron and 0.050 mg/L for manganese (Council, 1998; *Drinkwaterbesluit*, 2011). For instance, Vitens, the largest

drinking water company of the Netherlands, aims at keeping iron and manganese levels lower than 0.05 and 0.01 mg/L respectively. A common treatment process applied in The Netherlands to remove iron and manganese from groundwater is aeration combined with rapid sand filtration. Iron and manganese can be removed by three processes occurring in the sand filter: homogenous oxidation, heterogeneous oxidation and biological oxidation.

Homogeneous oxidation is the oxidation of Fe^{2+}/Mn^{2+} to $Fe^{3+}/Mn^{3+}/Mn^{4+}$ ions and the subsequent hydrolysis resulting in flocs that precipitate on and between the sand particles. Homogeneous oxidation is dominantly occurring in the zone where an oxidant is present and no adsorbent is present. In water treatment practice, homogeneous oxidation occurs predominantly in the supernatant layer of the pre-aerated submerged rapid sand filter (RSF), but also in the water phase of the filter bed. In contrast to homogeneous oxidation of iron, homogeneous oxidation of manganese in a rapid sand filter is negligible (Diem and Stumm, 1984). A filter which is continuously emptied via a free outflow and thus no supernatant is present, will be referred to as trickling filter. Since water is absent, there will always be air in the filter bed and oxygen depletion will not occur. Heterogeneous oxidation describes the process in which Fe^{2+}/Mn^{2+} sorbs to a surface area (e.g. hydrous ferric oxides) where it can subsequently be oxidized, resulting in the formation of new sorption sites. This process takes place mainly at the surface of the filter medium of submerged sand filters and trickling filters. The third mechanism of iron and manganese removal in sand filters is the biological oxidation of these compounds by iron and manganese oxidizing bacteria (IOB and MOB). A number of IOB have been reported in literature to be involved in the biological oxidation of iron, such as: *Leptothrix ochracea*, *Gallionella ferruginea, Toxothrix trichogenes, Thiobacillus ferrooxidans* and *Crenothrix* (Michalakos et al., 1997; Kirby et al., 1999; Sharma et al., 2005; Rentz et al., 2007). Similarly, several bacterial strains involved in the oxidation of manganese are found on filter grains and in the water phase and have been reported, like *Pseudomonas sp.*, *Streptomyces sp.*, and *Leptothrix sp.* (Bruins, 2016). Monod expressions to model growth rates of bacteria is the most common assumption to deal with biological activity (Liu et al., 2001; Aa et al., 2002), but as far as the authors are aware of, there are very little studies known in mathematically describing removal of iron and manganese by biological oxidation.

Iron and manganese removal in aeration and RSF has always been operated by drinking water treatment companies based mostly on experience and rules of thumb (Mouchet, 1992; Sommerfeld, 1999). Despite the wide-spread application of RSF for groundwater treatment in Western Europe, US and Canada, specific insights in the fundamental mechanisms (homogeneous, heterogeneous and biological oxidation) underlying the removal of iron and manganese in this process step as a function of changed process conditions and ground water composition is still lacking. Modelling these mechanisms provide means to test assumptions about mechanisms and compare model simulation results with measurements from groundwater treatment practice. Process optimization and advanced control of e.g. backwashing frequency can be supported (validated) by model simulations. For example, high supernatant levels, intensive aeration and high pH will result in a relatively high rate of homogeneous formation of iron oxides, thereby increasing the filter bed resistance. To prevent clogging of the filter, more frequent backwashing is needed and this will result in increased losses of backwash water. Heterogeneous oxidation leads to only minimal head loss, which indicates that heterogeneous oxidation is generally preferred over homogenous oxidation, especially where the heterogeneous oxidation rate becomes favorable when compared to the homogeneous or biological oxidation rate – e.g. in the case of anoxic groundwater with a somewhat alkaline pH (Sharma, 2001) and medium to high iron concentrations (Beek et al., 2012a). Due to continuous deposition of iron(III) hydroxides by

heterogeneous oxidation, the size of the iron(III) hydroxide filter grains will increase during RSF operation. The increase of filter grain size leads to a decrease of the specific surface area and an increase of the filter bed, which is also experienced in practice (Beek et al., 2012a). However, it is believed that microbiology can play a key role in the oxidation of iron (II), and it seems that depending on the exact circumstances, one of the three mechanisms is dominant (Beek et al., 2015).

Depending on the type of filtration used (trickling filters or submerged filters) and the contact time distribution with oxygen, the ratio of homogeneous versus heterogeneous oxidation can be different. Besides the concentration of manganese and iron, the type of filtration is largely dependent on the concentration of ammonium and/or methane (Vet et al., 2011). Another important aspect of removal efficiency is that many water quality parameters (e.g. pH, alkalinity, temperature, organic matter, Cu^{2+}, Co^{2+}, $H_2PO_4^-$) can affect iron and manganese removal (Stumm and Lee, 1961; Graveland, 1971; Theis and Singer, 1974; Sharma, 2001). Since the water quality can differ to a large extent between drinking water treatment plants, it is difficult to predict to what extent iron and manganese will be removed. Likewise, the number of processes involved are characterized by different time-scales (including distribution time affecting the amount of oxidation) and can influence one another.

Hence, a model describing these different mechanisms could potentially be used as an assessment tool for finding operational conditions or even be part of RSF process monitoring and control with the aim to maintain a desired level of filtrate quality while keeping the operational costs at a minimum. Most studies, e.g. (Ives, 1970; Schwager and Boller, 1997; Jegatheesan and Vigneswaran, 2005), with respect to iron and manganese removal in RSF treatment focus on physical and hydraulic aspects rather than changes of water quality due to chemical and biological reactions. Çakmakci et al. (2010) developed an artificial intelligence model for iron removal in sand filtration, based on a laboratory-scale experiment. However, such a model is difficult to interpret since it does not explicitly relate to (known) chemical, physical and biological reactions and mechanisms. A model that incorporates both hydraulic resistance, particle removal and chemical removal reactions, i.e. oxidation and adsorption, is described by (Teunissen, 2007). However, in this model changes in water quality due to chemical speciation (with e.g. carbonate ions) is not incorporated and adsorption isotherm values have not been determined from field data. In addition, equilibria reactions with iron and manganese hydroxides are not mass-balanced.

To overcome the aforementioned limitations, the main objective of this study is to develop a knowledge based model for iron/manganese removal in rapid sand filters to test and validate the assumed removal mechanisms by oxidation. Specifically, it is aimed to assess the following aspects: (1) the effect of pH and the height of the supernatant influent water layer on iron/manganese removal, (2) to apply Freundlich adsorption isotherm parameter values from batch-experiments for iron and manganese and compare these with other values in literature, (3) to validate model simulation results with field data obtained from different drinking water companies, calibrate and assess critical model parameters on iron and manganese removal. Pursuing these aims, the model needs to have enough degrees of freedom to cover different operational conditions but at the same time, not be over-parameterized in order to keep model validation feasible and keep the variance of model parameters at an acceptable level. Furthermore, modelling focus is set on submerged rapid sand filtration (i.e. there is supernatant layer on top of the filter medium) and treatment of groundwater with negligible amounts of methane and organic material.

2.2 Materials and methods

Assumptions have been made to model iron, manganese and ammonium removal. Material and methods relating to modeling assumptions are described in more detail in the section 'Model description'. For validation purposes, data is collected from literature and additional samples are taken from the influent water, filter media, and water collected at different bed heights at five Dutch water production sites. Adsorption isotherms of filter materials sampled from three Dutch production sites Holten and Spannenburg (Schoonenberg Kegel, 2015) and Velddriel (this work) are determined under anaerobic conditions to fix some degrees of freedom of the model. The RSFs of Velddriel contain two different filter media: a bottom layer of sand (bed height of approximately 1.8 m) and an upper layer of anthracite with a layer height of approximately 0.35 m. Samples from filter media of the pressurized RSF at the production site of Velddriel was determined at three different depths (i.e. the anthracite layer between 0.0 and 0.75m, the sand layer region between 1.0 and 1.5m, and another sample in the sand layer between 1.5 and 2.25m).

Sample collection, preparation and laboratory analysis is described below.

- *Glovebox experiments* were conducted to determine Freundlich adsorption isotherms of collected filter material samples under (near) anoxic conditions. Filter medium samples were collected from an operational sand filter at Velddriel at three different filter bed depths (0 – 0.5m, 0.75 – 1.25 m, and 1.50 – 2.0 m). Batches for the sorption experiment were prepared in a glovebox (Plexmaster Pro Quick, Ganuk GMBH) under anaerobic conditions by flushing the glovebox with nitrogen gas (99.9% pure, Linde gas). Oxygen was found to be lower than 60 μg/L solution during the experiments. Ten serum bottles (100 mL) were filled with filter medium (0.25, 0.5, 1.0, 1.5, 2.0, 3.0 and 4.0 gram, and 2 blanks without filter medium addition). Two serum bottles containing 0.25 gram of filter medium were prepared to check and correct for possible sample variation. Depending on characterization of iron or manganese adsorption, iron(II) sulfate heptahydrate (FeSO4.7H2O, Boom, The Netherlands, 123 mg) or manganese(II) chloride tetrahydrate (MnCl2.4H2O, Merck, The Netherlands, 44 mg) and sodium hydrogen carbonate (NaHCO3, JT Baker, The Netherlands, 1200 mg) were dosed in 2.4 kg Milli-Q water (pH was adjusted to 7.3 by adding HCl (1M) or NaOH (1M). The iron or manganese solution (100 mL) was added to all serum bottles. All serum bottles were mixed on magnetic stirrer (300 rpm, Variomag multipoint 6) in an incubator (10˚C, Hettich HettCube 400R). After 24 hours samples were taken and filtrated with 0.45 μm filters (Whatman Spartan 30/0.45 RC) under anaerobic conditions to determine the dissolved iron (II) and manganese (II) concentration. Oxygen was measured with an oxygen probe (Orbisphere model 26060 equipped with sensor 2110, Hach Lange, The Netherlands). pH was measured with a pH probe (Hach HQ 40d equipped with a PHC20101 sensor).
- *Laboratory chemical analyses* consisted of inductively coupled plasma mass spectrometry (ICP-MS) analysis of dissolved compounds. pH and oxygen were measured with online probes. Water was sampled from the anoxic source and at different heights of the pre-aerated RSF unit. Samples were taken at treatment plants that treat anoxic groundwater by aeration (plate aeration or direct oxygen intake) followed by fast filtration and conditioning. Only (pre-aerated) pre-filtration units were sampled. Most Dutch ground water treatment plants have treatment trains where a second filtration step takes care of manganese removal after conditioning by a softening step. An overview of the selected drinking water production sites and collected water quality parameters of the influent water is given in Table 2-1. Collected samples were analysed

with ICP-MS to determine the concentration of ferrous iron, manganese(II), phosphate, ammonium, nitrate and nitrite. ICP-MS was also used to determine the equilibrium concentrations obtained by the adsorption experiments.

TABLE 2-1: OVERVIEW OF WATER QUALITY PARAMETERS OF THE INFLUENT WATER OF GROUNDWATER PRODUCTION SITES APPLYING RAPID SAND FILTRATION.

	Fe^{2+}	Mn^{2+}	HCO_3^-	Ca^{2+}	Cl^-	Na^+	NH_4^+	pH	PO_4^-	O_2(aq)	T
Production site	mg/L	mg/L	mg/L	mg/L	mg/L	mg/L	mg/L	-	mg/L	mg/L	°C
Holten (pre-filters)	6.73	0.828	84.8	28.0	14.5	10.3	0.164	6.25	0.061	7.07	10.0
De Punt	5.42	0.202	120.5	66.2	38.0	24.1	0.406	7.07	0.805	10.00	10.5
Noordbargeres	14.1	0.498	120	56.1	28.0	19.1	0.228	6.91	0.512	10.00	12.0
Ossendrecht (pre-filters)	14.5	0.160	115	52.0	19.5	14.5	0.495	6.84	0.600	6.35	10.0
Velddriel (pre-filters)	3.59	0.469	361	113	21.0	12.8	1.400	7.35	0.880	10.80	11.0

2.3 Model description

The model for the removal processes in RSF comprises of two parts: (1) a section devoted to (homogeneous) removal of iron and manganese, ion speciation and mixing in the upper supernatant layer of the submerged RSF and (2) a part that describes iron, manganese and ammonium removal in the filter bed. Figure 2-1 schematically depicts these two model key components for describing the operation of RSF during runtime. Due to the key role of alkalinity, acidity and oxygen, chemical speciation software PHREEQC (Parkhurst and Appelo, 1999; 2013) is used to model the removal processes.

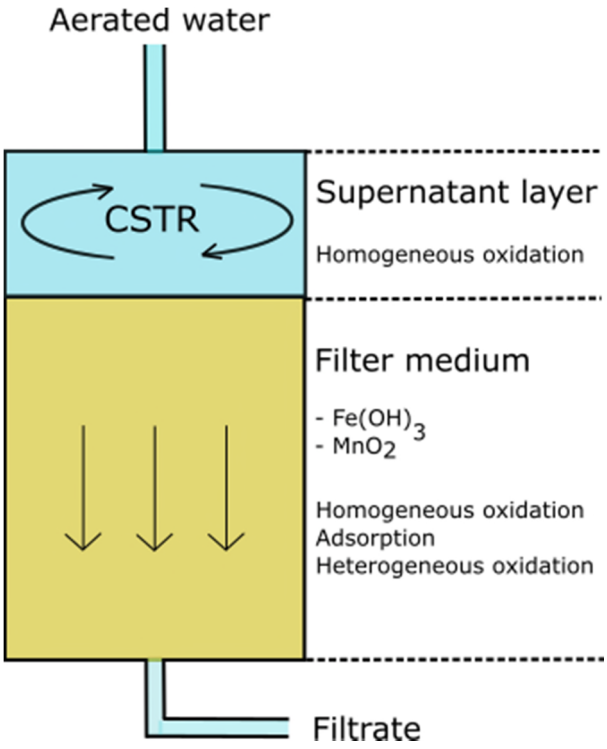

FIGURE 2-1: SCHEMATIC OVERVIEW OF KEY COMPONENTS IN THE RSF MODEL, WHERE AERATED WATER ENTERS THE RSF AND MIXES WITH THE SUPERNATANT LAYER.

Furthermore, the following assumptions are made:

- Homogeneous and heterogeneous oxidation are the only mechanisms considered that describe iron and manganese removal. Further assumptions and equations are described in a separately in section *Homogeneous oxidation* and *Heterogeneous oxidation*. Additionally, it is assumed that the accumulation of hydrous ferric oxides (HFO) is counteracted by a decrease of the available surface area ratio (versus filter particle volume) and flushing effects of backwashing.
- The amount of HFO is *equally distributed* over the filter bed height. For the Velddriel RSFs, a dual layered model is developed where it is assumed that iron oxide coated anthracite (IOCA) is present in the top layer and (iron oxide coated) sand (IOCS) in the bottom layer and IOCA and IOCS have different adsorption characteristics;
- *Clogging* of the filter and pressure build-up is not described;
- *Nitrification.* Removal of ammonium is assumed to only take place by ammonium oxidizing bacteria using an existing nitrification model, where the initial biomass concentration is equally distributed over the filter (Aa et al., 2002).

- Simple hydrodynamics, i.e. continuously stirred reactor *(CSTR) and advection-dispersion modelling*, that describe the water flow in, respectively, the upper, supernatant layer of the RSF and through the filter bed. Dispersion and CSTR modelling of the supernatant layer are tested and validated at a Dutch drinking water production site by spiking with a NaCl solution (Schoonenberg Kegel, 2013). The water flow through the filter bed is assumed to follow advection – (turbulent) dispersion dynamics where the advection velocity is calculated with the aid of porosity and the filtration flow;
- Iron and manganese are represented as either being dissolved as Fe(II) and Mn(II) ions, being bound to adsorbent filter material or as being oxidized to ferric iron and hydrolised ($Fe_2(OH)_3$) or completely oxidized to Mn(IV) (and hydrolyzed to MnO_2), respectively.
- Surface complexation by the double-layer concept (Dzombak and Morel, 1990) using charge interaction forces and strong and weak binding sites is simplified by considering only strong sites and modifying the surface species equilibria reactions by adsorption equilibria using Freundlich isotherm values, see section *Heterogeneous oxidation* for more details. For dual media RSFs, two different species are defined in PHREEQC to allow the inclusion of different, experimentally determined adsorption characteristics of the anthracite and sand filter layer.
- Analogously to the definition of ammonium ions, Fe(II) and Mn(II) is considered as a separate species to circumvent speciation to their oxidized form and allow for kinetic reactions. Kinetic rates for homogeneous and heterogeneous are included in the PHREEQC database. For dual media filters (e.g. the Velddriel production site), rates are defined per layer medium.

2.3.1 Homogeneous oxidation

Homogeneous oxidation of iron is described in a simplified manner by equations describing oxidation and hydrolysis (Sung and Morgan, 1980; Tamura et al., 1980; Beek et al., 2012a):

Oxidation: $Fe^{2+} + \frac{1}{4}O_2 + H^+ \rightarrow Fe^{3+} + \frac{1}{2}H_2O$ (1a)

Hydrolysis: $Fe^{3+} + 3H_2O \rightarrow Fe(OH)_3 \downarrow + 3H^+$ (1b)

Leading to the overall reaction: $Fe^{2+} + \frac{1}{4}O_2 + 2\frac{1}{2}H_2O \rightarrow Fe(OH)_3 \downarrow + 2H^+$ (1c)

The formed hydrous ferric oxide (HFO, $FeOH_3$) is assumed representative of all hydrous ferric oxides that can potentially be formed (e.g. FeOOH). The reaction rate of homogeneous oxidation is described by a kinetic rate (Beek et al., 2012b) where the rate of Fe(II) removal is dependent on Fe(II), oxygen and pH:

$$\frac{d}{dt}[Fe^{2+}] = -k_{Fe,hom}\frac{[Fe^{2+}][O_2]}{[H^+]^2} \quad (2)$$

The reaction rate constant is determined at $2.20 \cdot 10^{-15}$ M^{-2} s^{-1} with the aid of different residence times and measurements of ferric iron (Beek et al., 2012b). This value is used for all the simulations in this work and in range with the range reported by .

Homogenous oxidation of manganese is written analogously:

$Mn^{2+} + \frac{1}{4}O_2 + H^+ \rightarrow Mn^{3+} + \frac{1}{2}H_2O$ (3a)

$Mn^{3+} + \frac{1}{4}H_2O + H^+ \rightarrow Mn^{4+} + \frac{1}{2}H_2O$ (3b)

$$Mn^{2+} + \frac{1}{2}O_2 + 2H^+ \rightarrow Mn^{4+} + H_2O \quad (3c)$$

Subsequently, Mn^{4+} is hydrolyzed to MnO_2 (in solid form). It is further assumed that the oxide MnO_2 is representative of all manganese oxides that can be formed, like Mn_3O_4 and MnOOH:

$$Mn^{4+} + 2H_2O \rightarrow MnO_2 \downarrow + 4H^+ \quad (4)$$

The reaction rate constant is determined according to:

$$\frac{d[Mn^{2+}]}{dt} = -k_{Mn,hom}[OH]^{2.56}[Mn^{2+}] \quad (5)$$

For the reaction constant $k_{Mn,hom}$ a value of $2.08 \cdot 10^{-2}$ $(mol/L)^{-2.56}$ s^{-1} is adopted (Davies and Morgan, 1989) which has been determined at 298 K. Indeed, this constant – also after a correction to groundwater temperature by the aid of the Arrhenius equation - leads to a half time removal of Mn(II) in the order of years (Diem and Stumm, 1984) and is therefore negligible compared to the half time of the heterogeneous oxidation rate of manganese.

2.3.2 Heterogeneous oxidation

Heterogeneous oxidation of iron is considered as sorption of ferrous iron onto a surface area such as iron coated sand (IOCS) followed by oxidation and hydrolysis (Sung and Morgan, 1980; Tamura et al., 1980; Beek et al., 2012a):

$$HFO - OH + Fe^{2+} = HFO - OFe(II)^+ + H^+ \quad (6a)$$

$$HFO - OFe(II)^+ + \frac{1}{4}O_2 + H^+ \rightarrow HFO - OFe(III)^{2+} + \frac{1}{2}H_2O \quad (6b)$$

$$HFO - OFe(II)^{2+} + 2H_2O \rightarrow HFO - OFe(III)(OH)_2 + 2H^+ \quad (6c)$$

Leading to:

$$HFO - OH + Fe^{2+} + \frac{1}{4}O_2 + \frac{3}{2}H_2O \rightarrow HFO - OFe(III)(OH)_2 + 2H^+ \quad (6d)$$

Where oxidation kinetics are driven by the presence of oxygen and adsorbed ferrous iron, assuming the amount of HFO surface sites constant:

$$\frac{d[Fe(II)_{ads}]}{dt} = -k_{\mathrm{Fe,\,het}}[\mathrm{Fe}(II)_{ads}][O_2] \quad (7)$$

The amount of adsorbed iron(II) is defined to sorb to strong sites of HFO (HFO_s) according to an equilibrium following the Freundlich isotherm convention: $HFO_s + (1/n)Fe^{+2} = HFO_s\text{-}Fe$. Note that this way, the equilibrium equation becomes mass unbalanced which can be an issue for speciation tools if no measures are taken (in PHREEQC, these measures are the no-check and mole-balance options[4]). Rewriting the thermodynamic solubility equilibrium constant, we can calculate the amount of adsorbed Fe^{+2}:

[4] Notice that, to circumvent charge imbalances in PHREEQC when calculating the equilibrium at the surface, the proton is accounted for in PHREEQC code describing the kinetic rate Eq. (7).

$$\mathrm{Fe}(II)_{\mathrm{ads}} = K_{\mathrm{Fe}} m_{\mathrm{HFO}} [\mathrm{HFO}][\mathrm{Fe}^{+2}]^{1/n} \quad (8)$$

Note that substitution of Eq. (8) in Eq. (7) leads to a product of the heterogeneous oxidation constant $k_{\mathrm{Fe,\,het}}$ and the Freundlich constant $K_{\mathrm{Fe,\,het}}$, as has also been observed by previous authors (Tamura et al., 1976; Sung and Morgan, 1980; Tamura et al., 1980). We calibrated $k_{\mathrm{Fe,\,het}}$ to a value of 3.0 M^{-1} s^{-1} for the Holten case, for other production sites we use the value obtained by Tamura et al. (1976) (i.e. 73.0 M^{-1} s^{-1}). Apparently, the conditions of the Holten RSF case (slightly acidic) slows the reaction more than theoretically predicted. For the Velddriel RSF case, a new surface species for anthracite is introduced in PHREEQC with Freundlich constants $K_{\mathrm{Fe,anthr}}$ and $1/n_{\mathrm{anthr}}$ as determined by the glovebox experiment with the sampled material of the upper layer. For HFO (the sand layer), the Freundlich value corresponding to the middle layer is used since the bottom (sand) layer had very little adsorption capacity compared to the middle layer. For the Velddriel case, it is assumed that for iron oxide coated anthracite (IOCA) and IOCS, the heterogeneous iron oxidation rate has the same value.

Assuming there is a sufficiently large amount of HFO present, the amount and concentration of adsorbent will not change significantly when an RSF is operational and filter medium particles are coated with iron and manganese oxides. Hence we assume the product $m_{\mathrm{HFO}}[\mathrm{HFO}]$ to be a fixed constant, such that the calculation of the Freundlich constant K_{Fe} will not be dependent on filter operation (simulated) time.

Heterogeneous oxidation of manganese is similar to heterogeneous iron oxidation, with the exception that manganese can adsorb onto both birnessite as well as iron hydroxides (IOCS). In the model, birnessite $(Na_{0.3}Ca_{0.1}K_{0.1})(Mn^{4+},Mn^{3+})_2O_4 \cdot 1.5\ H_2O$ is simplified to MnO_2. In PHREEQC, this leads to the introduction of birnessite as a new surface species (e.g. BIRN) and two equilibrium equations: HFO + $(1/n)Mn^{+2}$ = HFO-Mn^{+2} and BIRN + $(1/n)Mn^{+2}$ = BIRN-Mn^{+2}.

Furthermore, analogously to Eq. (7), the heterogeneous reaction rate is expressed as being dependent on the amount of adsorbed manganese(II) and the partial pressure of oxygen (pO_2) under (near) atmospheric conditions:

$$\frac{d[Mn(II)_{ads}]}{dt} = -k_{het,\mathrm{Mn}}[\mathrm{Mn}(II)_{ads}][O_2] \quad (9)$$

For the heterogeneous manganese rate constant ($k_{\mathrm{het,\,Mn}}$), a value of $2.4 \cdot 10^{-4}$ M^{-1} s^{-1} is assumed (Davies and Morgan, 1989) for manganese oxide coated sand (MOCS), unless stated otherwise. For several production sites, the heterogeneous manganese oxidation rate is allowed to vary for manganese oxide coated anthracite (MOCA) and for MOCS. The calibrated values are listed in Table 2-1. Again, similar to the iron heterogeneous case, the adsorbed amount of manganese is dependent on the amount of adsorbent ($m_{\mathrm{adsorbent}}$), being birnessite or HFO:

$$\mathrm{Mn}(II)_{\mathrm{ads}} = K_{\mathrm{Fe}} m_{\mathrm{adsorbent}} [HFO, \mathrm{Birn}][\mathrm{Mn}]^{1/n} \quad (10).$$

TABLE 2-2: OVERVIEW OF HETEROGENEOUS OXIDATION CONSTANTS USED TO SIMULATE GROUNDWATER PRODUCTION SITES APPLYING RAPID SAND FILTRATION. PAF: PRE-AERATED FILTER. VALUES OBTAINED FROM LITERATURE ARE TYPESET IN BOLDFACE.

	$k_{het,Fe}$	$k_{het,Mn}$ (sand)	$k_{het,Mn}$ (anthracite)

	$M^{-1}\ s^{-1}$	$M^{-1}\ s^{-1}$	$M^{-1}\ s^{-1}$
De Punt	0.73	**$2.40 \cdot 10^{-4}$**	n.a.
Holten (PAF)	3.00	$2.40 \cdot 10^{-6}$	n.a.
Ossendrecht (PAF)	0.73	$7.00 \cdot 10^{-5}$	n.a.
Noordbargeres	0.07	$2.00 \cdot 10^{-3}$	n.a.
Velddriel (PAF)	**73.0***	$2.00 \cdot 10^{-3}$	$2.40 \cdot 10^{-6}$

*The value for the heterogeneous oxidation constant at production site Velddriel is assumed the same for IOCS and IOCA.

2.3.3 Data from drinking water production sites

For validation purposes, data was collected from literature and additional samples were taken from the influent water, filter media, and water collected at different bed heights from well performing Dutch water production sites. Main process characteristics per production site are listed in Table 2-3.

TABLE 2-3 OVERVIEW OF PROCESS CONDITIONS OF AEARATED GROUNDWATER PRODUCTION SITES APPLYING RAPID SAND FILTRATION. PAF: PRE-AERATED FILTER. SN: SUPERNATANT LEVEL.

	SN level	**Bed height**	**Superficial flow velocity**	**Bed contact time**
	m	m	m/h	min
De Punt	1.0	2.3	4.4	12.5
Holten (PAF)	0.3	2.3	23.3	2.9
Ossendrecht (PAF)	0.5	2.0	7.5	6.2
Noordbargeres	0.1	2.0	4.7	9.6
Velddriel	0.3	2.1	5.1	9.6

2.4 Results and discussion

2.4.1 Homogeneous oxidation

2.4.1.1 Iron and manganese removal in the supernatant layer

The effect of the supernatant layer height on Fe^{2+} removal is simulated for the Velddriel RSF case and is presented in Figure 2-2 (simulation results depicted in blue, measurements are depicted as grey markers). Please note that an increase of the supernatant layer height removes the influent iron(II) concentration considerably, to a value of 3.1 mg/L for a supernatant layer of 80 cm (dotted black line). For a supernatant layer of 27 cm, this decrease in iron concentration is smaller and is equal to 0.17 mg/L (from 3.5 mg/L to 3.33 mg/L) and for a supernatant layer of 10 cm the decrease in iron is only 0.05 mg/L. The higher iron removal for a higher supernatant layer follows from the fact that an increase in the height of the supernatant layer results in an increased residence time and thus more oxidation time. Notice that the (effect of supernatant layer height on) manganese removal is negligible.

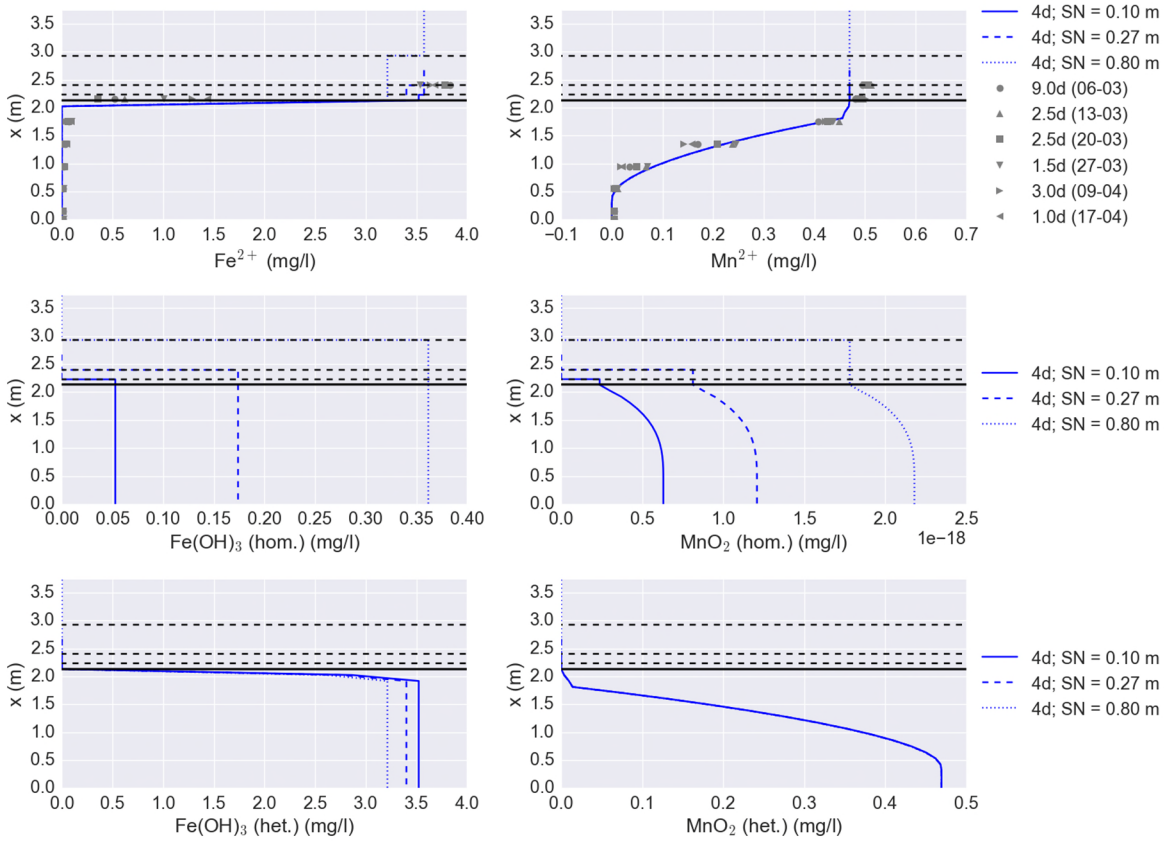

FIGURE 2-2: EFFECT OF SUPERNATANT (SN) LAYER HEIGHT ON METAL ION CONCENTRATIONS AND METAL OXIDES FORMED BY OXIDATION ACROSS THE RSF (HEIGHT MEASURED FROM THE BOTTOM, FILTRATION TIME IS SET AT 4 DAYS). FIRST ROW: FE(II) AND MN(II) CONCENTRATIONS (MEASURMENTS ARE SHOWN AS GREY MARKERS AND ARE LABELED WITH THE FILTRATION TIME AND SAMPLING DATE), SECOND ROW: HOMOGENEOUSLY FORMED IRON OXIDE (LEFT) AND MANGANESE OXIDE (RIGHT), THIRD ROW: HETEROGENEOUSLY FORMED IRON OXIDE (LEFT) AND MANGANESE OXIDE (RIGHT).

2.4.2 Heterogeneous oxidation

2.4.2.1 Freundlich parameters

Freundlich parameters were collected and recalculated from literature or were determined for iron and manganese adsorption on collected filter medium samples from an RSF unit in Velddriel. Collected values are presented in Table 2-4.

From Table 2-4 it is observed that Fe(II)/Mn(II)-sorption capacity is the largest in the top of the filter and smallest at the bottom of the filter at location Velddriel. The Holten pre-filters have the largest Fe(II)/Mn(II)-sorption capacity, while Velddriel (bottom of the filter 1.5-2.25 m) has the lowest sorption capacity for Fe(II) and Mn(II). Thus, Fe(II)/Mn(II)-sorption capacity can be different between filter locations or within a filter of a specific location as a function of filter depth.

Reference adsorption capacity for iron and manganese as adsorbate are calculated on the basis of 10.0 mg/l Fe(II) and 1.00 mg/l Mn(II) and with the aid of the Freundlich isotherm equations. Figure 2-3 presents a log-scale plot of the pH versus the sorbed amount of iron/manganese.

Clearly, across different collected filter medium samples, sorption capacity increases with higher pH values measured in water and can be reasoned by the adsorption (solubility) equilibrium equation which is pH dependent. It is well known that heterogeneous oxidation improves for a higher pH (Sharma, 2001; Buamah, Petrusevski, and Schippers, 2009; Beek et al., 2012a), because more binding sites of iron and manganese oxides become available for sorption of iron and manganese.

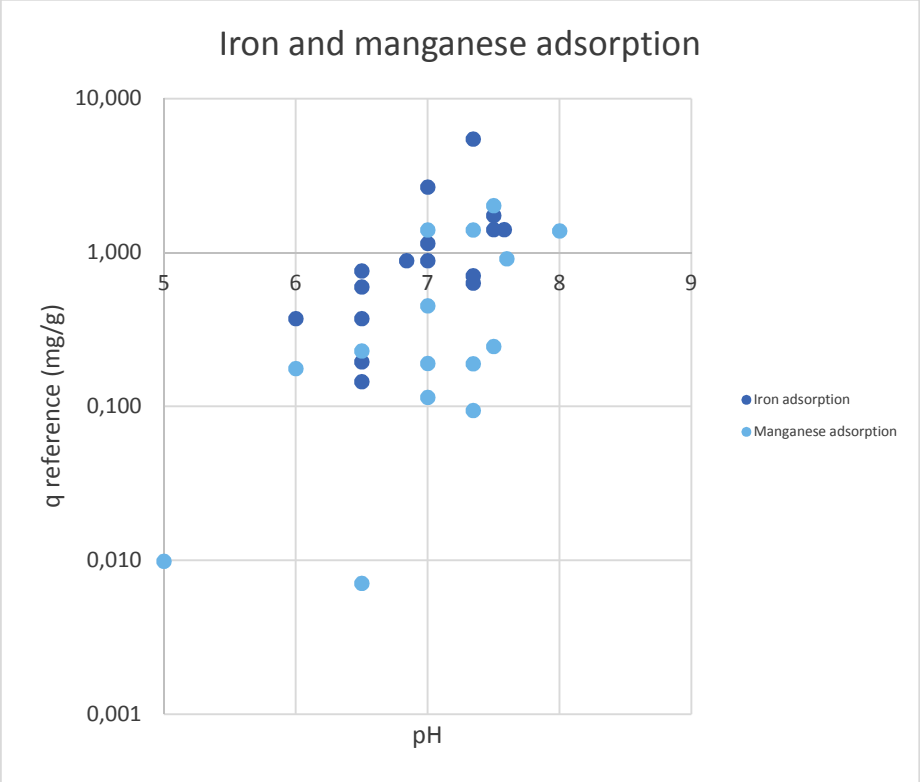

FIGURE 2-3: LOG10-SCALE PLOT OF SORBED IRON AND MANGANESE VERSUS PH, ON THE BASIS OF AN ADSORBATE CONCENTRATION OF 10.0 MG/L AND 1.00 MG/L FOR IRON AND MANGANESE RESPECTIVELY

2.4.2.2 Effect of amount of heterogeneous oxidation

The Freundlich values shown in Table 2-4 for the pre-aeration filters at production site Velddriel are used to simulate the iron and manganese profiles across the filter bed. Figure 2-4 shows simulated and measured bed profiles for the Velddriel case (dual layer filter) and Figure 2-5 shows (simulated) pH effects for the Holten production site.

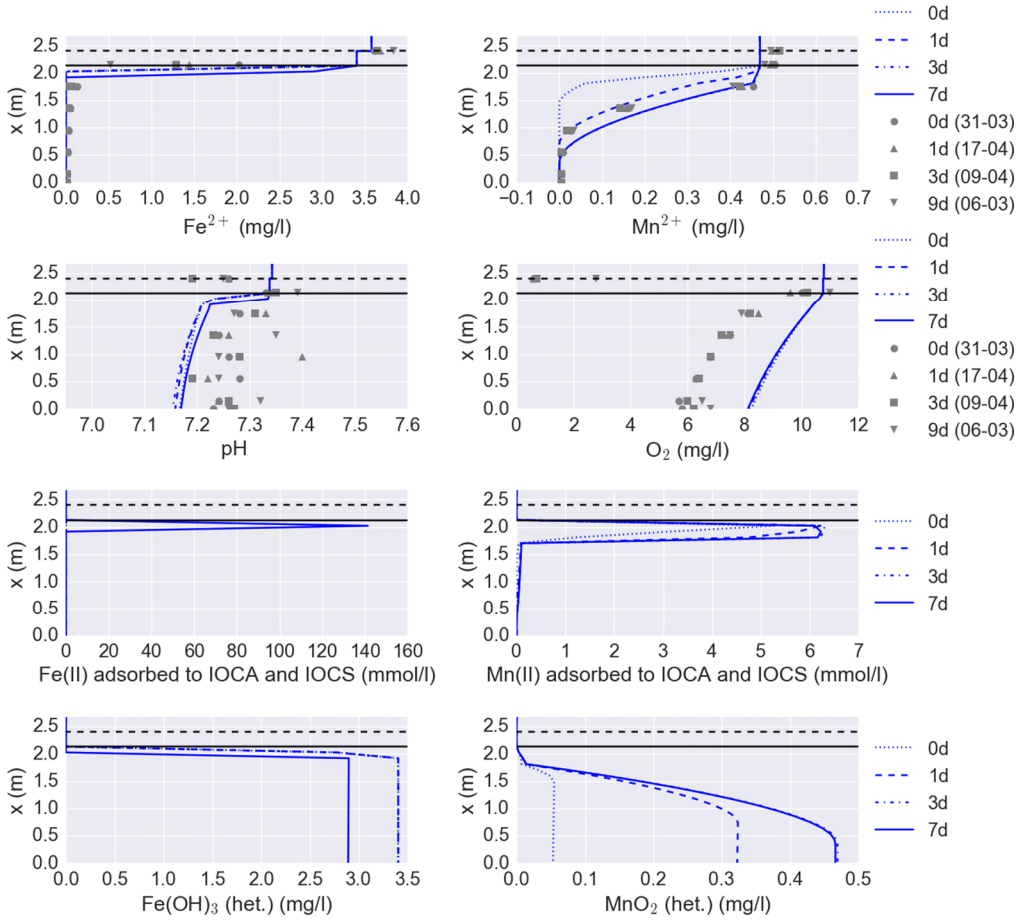

FIGURE 2-4: CONCENTRATION PROFILES OF IRON(II) AND MANGANESE(II) (UPPER ROW), PH AND OXYGEN LEVELS (2ND ROW), AMOUNT OF ADSORBED IRON(II) AND MANGANESE(II) (THIRD ROW) AND HETEROGENEOUSLY FORMED IRON AND MANGANESE OXIDES (4TH ROW); ALL SIMULATED (BLUE LINES) AFTER 0.5, 1, 3 AND 7 DAYS OF FILTRATION RUN TIME. MEASUREMENTS ARE MARKED GRAY.

Modeled iron(II) shows a sharp decline over a region of a few centimeters throughout the filter run time. However, the simulated decline is hard to validate with these measurements alone due to higher sample variation than usual, because the measurement sampling point was approximately at the boundary of supernatant layer and filter bed, making it uncertain whether heterogeneous oxidation might have occurred or not. The sharp decline in the prediction of pH at approximately 1.8 m filter bed height occurs simultaneously with the removal of iron and manganese, corresponding with the release of protons during heterogeneous oxidation. Hence, (changes in) pH is an important indicator of filtration efficiency, since iron/manganese removal is highly sensitive to changes in pH (Figure 2-5, 2nd from top, left hand side). It seems that pH is underestimated by the model of Velddriel (Figure 2-4). It is hypothesized that the under-estimation is a result of an overestimated rate of heterogeneous iron oxidation (not calibrated, see Table 2-2). A similar under-estimation is also observed in the Ossendrecht case (see supplementary material, Figure 0-6). Unfortunately, pH measurements show large variation among the collected samples, making validation of modeled results by pH alone not feasible.

From the same figure (Figure 2-4, top left panel), please note that the simulated iron concentration profile is hard to validate with the current data: the measured values of iron(II) vary considerably at a height of approximately 2.0 m from the bottom (just below the supernatant layer) while the model shows a sharp decline in iron concentration just a little bit further below in the filter, at approximately 1.8 m. Hence it is unsure whether homogeneous or heterogeneous oxidation by the model is under- or overestimated or whether the measurement uncertainty is higher than average (measurement uncertainties might be attributed to either mixed sampling of the boundary layer between supernatant and (anthracite) filter layer, or variation in residence times between the instant of sampling and adding acid to stop further oxidation). Furthermore, the decrease in oxygen seems to be underestimated by the model (Figure 2-4, 2nd from top, right hand side), which might be attributed to (i) the presence of oxygen depleted pockets in the filter which is not accounted for in the model or (ii) (more) oxygen is consumed by bacteria (e.g. nitrifying bacteria).

Remarkably, the modeled adsorption of manganese(II) occurs in the upper anthracite layer almost exclusively (Figure 2-4, 3rd row,right panel), but measurements indicate that removal takes place in the region 0.8 to 1.8 m (measured from the bottom of the RSF. Manganese adsorption as modeled with Freundlich parameters determined with a 'freshly' replaced filter material (samples taken at 06-03-2015) indicate further that only the upper anthracite layer adsorbs considerably (see also Figure 0-7 in section III of the supplementary material). The model predicts that within one day, this layer is over-saturated and breakthrough will occur. Most likely, the filter material 'ripens' during startup by biological activity, increasing the manganese removal capacity (Bruins, 2016) and hence having an effect on both the heterogeneous rate due to biological catalysis as well as the Freundlich adsorption isotherm values due to manganese oxides with different properties. Indeed, simulations show that a larger value than the heterogeneous rate constant reported in literature by Davison and Seed (1983b). In tandem, it is likely that more manganese oxide coated sand (MOCS) will be present in the region below the anthracite layer as a result of (biological) oxidation of manganese, which will improve manganese(II) adsorption further. A similar phenomenon was observed for production site Noordbargeres, where the same value of $k_{het,Mn}$ showed a good fit with the data.

TABLE 2-4: FREUNDLICH ISOTHERM CONSTANTS FOR IRON AND MANAGANESE ADSORPTION. PAF: PRE-AEREATED PREFILTERS. Log(K_p) IS THE LOGARITHM OF THE SOLUBILITY CONSTANT THAT IS USED IN THE PHREEQC MODEL.

Fe adsorption on IOCS	K (g/g) / (g/L)^1/n	1/n	Reference	Remark
Holten (pre-filters)	0.107	1.230	Schoonenberg, 2015	Isotherm determined for pH 6.5
Noordbargeres	0.006	0.430	Sharma, 1999	Validation of model with Gilze sand (Sharma 1999)
Ossendrecht (P.A.F.)	0.038	0.76	Schoonenberg, 2015	Simulation of model with Holten isotherm (pH 7.0)
Velddriel (PAF, anthracite) (0 - 0.75m)	0.066	0.540	This study	Isotherm determined for pH 7.3
Velddriel (PAF, sand) (1.0 - 1.5m)	0.002	0.225	This study	Isotherm determined for pH 7.3
Velddriel (PAF, sand) (1.5 - 2.25m)	0.002	0.228	This study	Isotherm determined for pH 7.3
Mn adsorption on IOCS				
Holten (pre-filters)	1.905	1.810	Schoonenberg, 2015	Isotherm determined for pH 6.5
Noordbargeres	0.043	0.495	Sharma, 1999	Validation of model with Gilze sand (Sharma 1999)
Ossendrecht (PAF)	0.081	0.95	Sharma, 1999	Simulation of model with Holten isotherm (pH 7.0)
Velddriel (PAF, anthracite) (0 - 0.75m)	0.026	0.814	This study	Isotherm determined for pH 7.3
Velddriel (PAF, sand) (1.0 - 1.5m)	0.018	0.369	This study	Isotherm determined for pH 7.3
Velddriel (PAF, sand) (1.5 - 2.25m)	0.006	0.507	This study	Isotherm determined for pH 7.3

2.4.2.3 Effect of pH

Figure 2-5 presents the simulated effect of pH of the influent water (and adsorption isotherms determined with the corresponding pH) on iron(II) and manganese(II) concentration, the pH and oxygen profile across the filter bed height and the amount of adsorbed iron(II) and manganese(II). Notice from the adsorbed amount of iron and manganese and their corresponding concentration profiles that removal is typically improved at higher pH (around 7.5), for manganese this effect in pH between 7 and 7.5 is very pronounced. This corresponds to earlier findings (Sung and Morgan, 1980; Beek et al., 2012a). Since the pH determines the reaction rate and proton exchange occuring during oxidation, it follows that the pH decreases during iron and manganese removal - its decrease proportional to the oxidation rate.

Biological oxidation seems to play a dominant role at pH 7.5 (Beek, 2015), however, research that confirms *into what extent* biology contributes in the removal of iron and manganese is still lacking. Since the pH at location Holten is approximately 6.5, the contribution of catalyzed - possibly biologically - oxidation is expected to be small. Remarkably, the ferrous heterogeneous oxidation rate calibrated for Holten is 20 times smaller than the value reported by Tamura et al. (1976) in literature. Low values are also found for the other production sites (De Punt, Ossendrecht and Noordbargeres) where pH is smaller than approximately 7.0. Biological effects were outside the scope of this study.

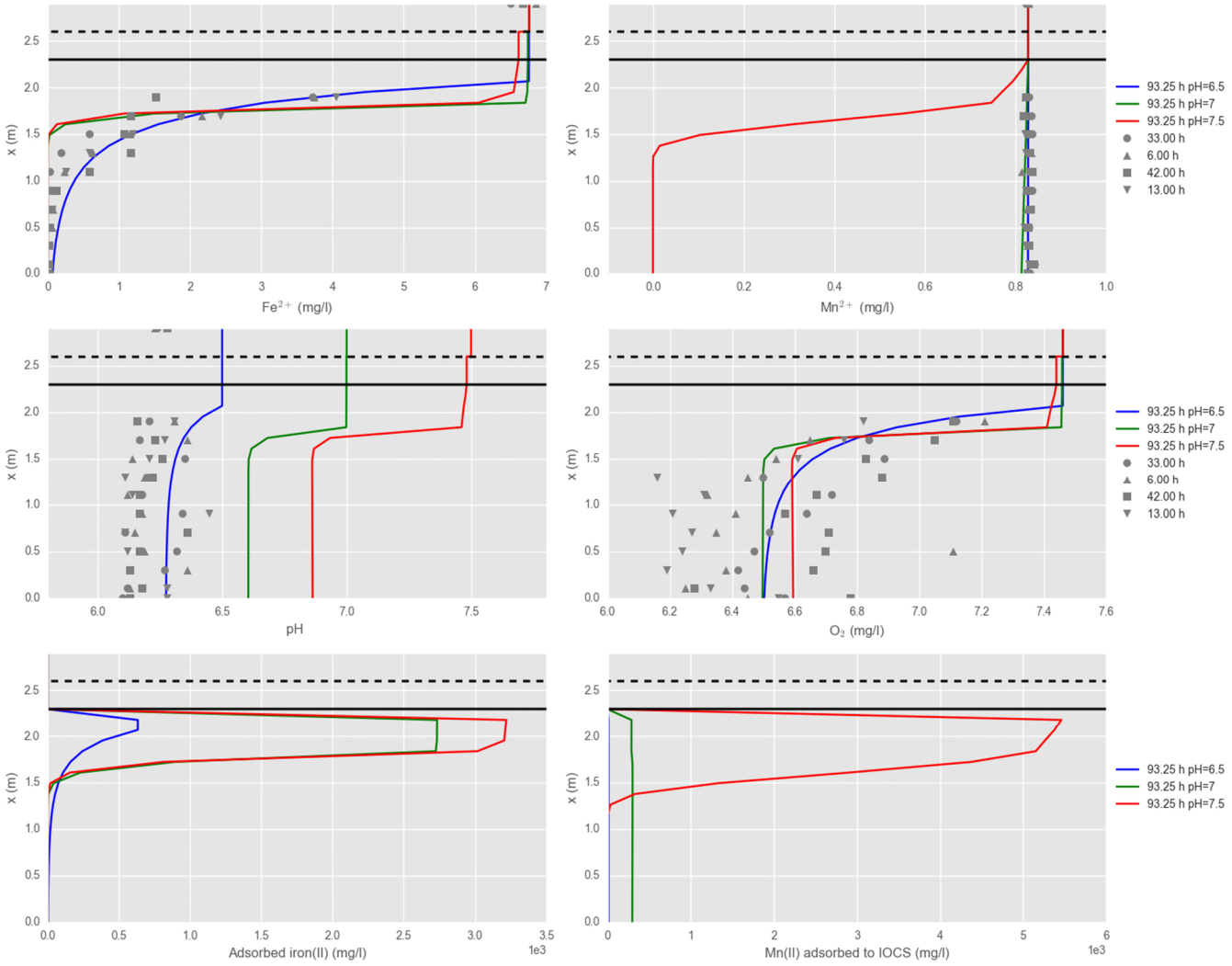

FIGURE 2-5 SIMULATED VALUES (COLORED LINES) AND SAMPLES TAKEN AT PRODUCTION SITE HOLTEN AT DIFFERENT TIMES DURING FILTRATION (GREY MARKERS). SIMULATION IS PERFORMED WITH FREUNDLICH VALUES OBTAINED UNDER DIFFERENT ACIDIC CONDITIONS. IN PRACTICE, THE PH IS APPROXIMATELY 6.5.

2.4.3 Validation with field data for homogeneous and heterogeneous oxidation

For both iron(II) and manganese(II), measured values are compared with simulated values using scatter diagrams, see Figure 2-6 and Figure 2-7. For water production plants Ossendrecht, De Punt and some data of production plant Holten (PAF), the simulations show good agreement with the measured values of iron(II). Please note that most of the other RSF cases show that the model underestimates the iron(II) concentration after RSF, even when the value of the heterogeneous iron oxidation constant is tuned. The Velddriel RSF case is illustrative for the need of calibration in the manganese case: the manganese heterogeneous oxidation rate is necessary to fit the model predictions to values from practice. Calibration to the Velddriel data results in a higher heterogeneous oxidation for MOCS ($2.0 \cdot 10^{-3}$ s^{-1}) and a lower value of heterogeneous oxidation rate for MOCA ($2.4 \cdot 10^{-6}$ s^{-1}) than reported in literature ($2.4 \cdot 10^{-4}$ s^{-1}, MOCS) and could be attributed to manganese oxidizing bacteria (Bruins, 2016). Notice that there is considerable variation in measurement data of notably iron(II) concentrations (Noordbargares data set 1 and 2, Holten (Figure 2-5) and Velddriel (Figure 2-4), hampering calibration of the heterogeneous iron oxidation constant. The cause of this variation could have been attributed to variation in timing to add acid to the samples to stop further oxidation, however, it is not verified further whether this was indeed the case.

Furthermore, note that results may deviate if other filtration times are assumed (see Figure 2-4 and the supplementary material, III) or if the isotherm constants are different than assumed. The results in Figure 2-6 and Figure 2-7 show that, iron and manganese removal can be predicted for most production sites. As a

recommendation for model validation, it is worthwhile to determine the removal capacity of different RSFs by sampling the influent and filtered water at different depths, perform biological analyses such as qPCR (polymerase chain reaction) to investigate amongst others nitrification and to determine adsorption and heterogeneous oxidation characteristics of the different filter materials at different depths. An alternative approach is to calibrate unknown model parameters, like the Freundlich constants for iron and manganese oxides and heterogeneous oxidation rates, to measurement data collected at different filtration run times and at different depths.

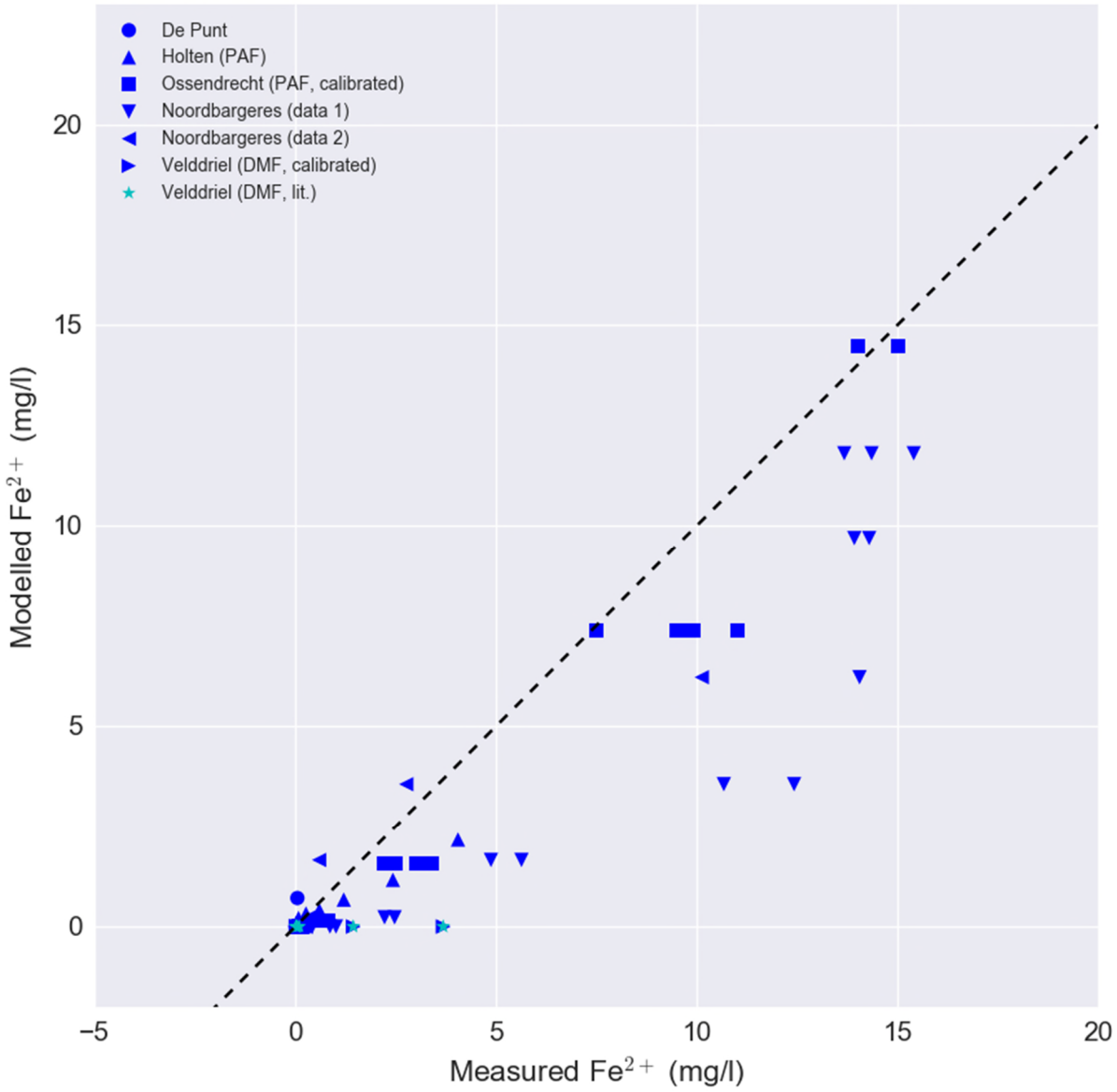

FIGURE 2-6: MODELLED VERSUS MEASURED IRON(II) IONS FOR DIFFERENT WATER PRODUCTION PLANTS. FOR PRODUCTION SITE VELDDRIEL

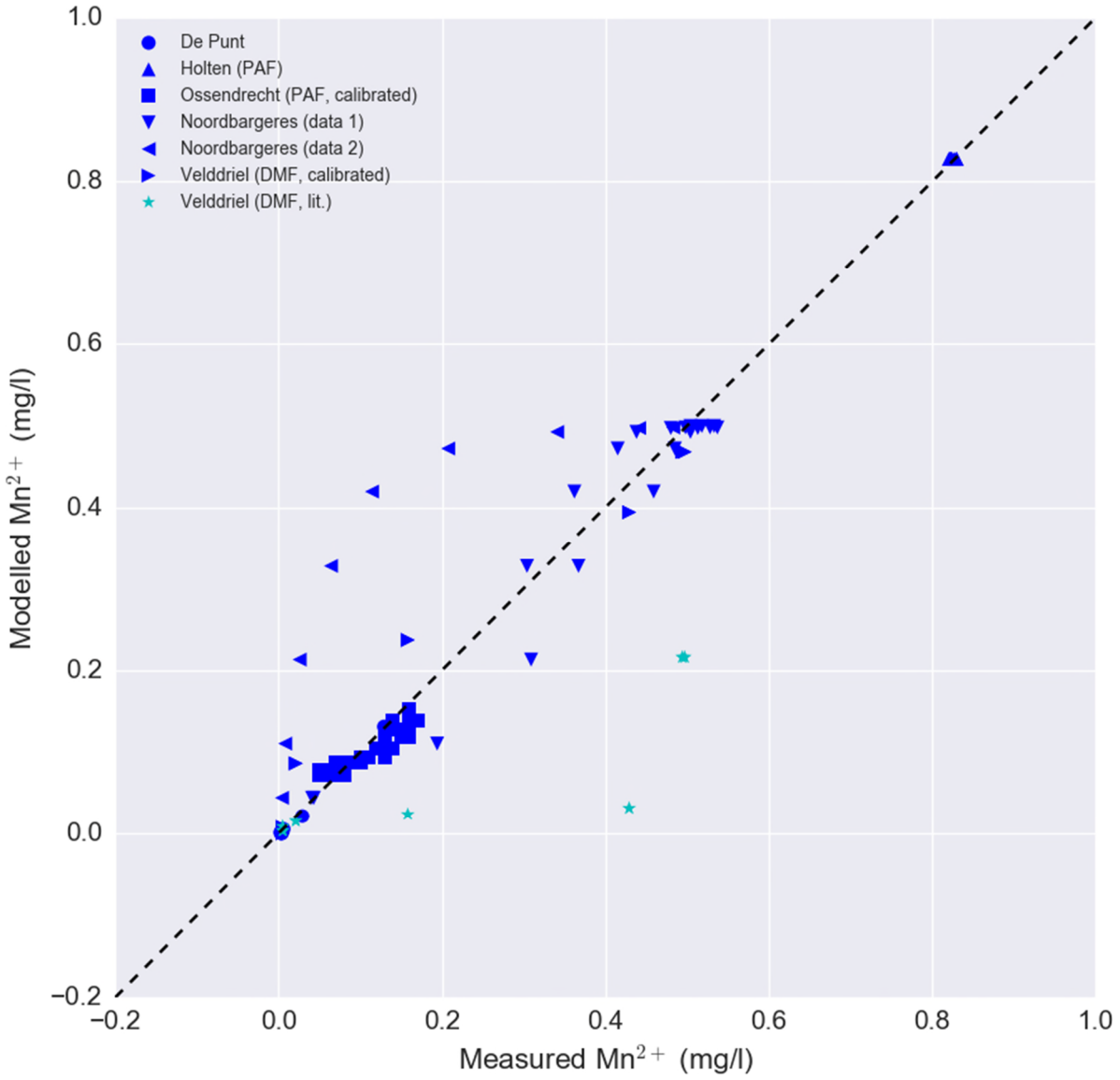

FIGURE 2-7: MODELLED VERSUS MEASURED MANGANESE(II) IONS FOR DIFFERENT WATER PRODUCTION PLANTS. FOR PRODUCTION SITE VELDDRIEL, CALIBRATED (HOLTEN: PYRAMID MARKER AND VELDDRIEL DUAL MEDIA FILTER: SQUARED MARKER) AND LITERATURE VALUES (DE PUNT: ROUND MARKER AND VELDDRIEL DMF: INVERTED PYRAMID MARKER) FOR THE HETEROGENEOUS MANGANESE OXIDATION RATE CONSTANT ARE USED.

2.5 Conclusions

A model has been developed that takes into account the main characteristics of (submerged) rapid filtration, a treatment configuration that is frequently applied in the Netherlands:

1. The effect of pH and distribution time in the supernatant layer on iron/manganese removal shows that, with different pH of the influent water (and determined isotherm model parameters at the corresponding pH) removal improves with increasing pH and the height of the supernatant layer positively influences the homogenous oxidation of iron(II). For manganese this improved removal effect is even more pronounced, most probably because iron will be removed in the upper RSF layer, thus not competing with manganese in adsorption and subsequent heterogeneous oxidation. For manganese, the effect of a higher supernatant layer has, as expected, a negligible effect on (homogeneous) removal;
2. By analysis of Freundlich adsorption isotherm values determind by batch experiments and values found in literature, it appears that sorption capacity of iron and manganese can differ significantly within a filter as function of filter depth (higher sorption capacity at the top compared to the bottom), but also between filters of different treatment plants. Sorption capacity generally increases with increasing pH;
3. Assessment of model simulation results with measurement data obtained from different drinking water production sites show that the heterogeneous oxidation rate and thus the adsorption isotherm values and the heterogeneous oxidation rate constant are critical model parameters for iron and manganese removal, and to a lesser extent, to filtration time. Since the heterogeneous oxidation process is (amongst others) dependent on the adsorbed amount of iron(II) and manganese(II) ions on IOCS and MOCS, it starts as soon as these ions get adsorbed. When heterogeneous (iron) removal is taking place, the pH drops which will slow down iron and manganese removal. The value of the iron and manganese heterogeneous constant of (iron or manganese) oxide coated sand was found to vary considerably across different Dutch drinking water production sites. The heterogeneous iron oxidation rate is lower than expected for several production sites where pH is smaller than 7.0, e.g. Holten (3.0 M^{-1} s^{-1}), Noordbargeres (0.0037 M^{-1} s^{-1}) and Ossendrecht (0.73 M^{-1} s^{-1}). For the double layer RSF at the production site Velddriel, the manganese heterogeneous oxidation constant for the MOCS layer was calibrated to be an order of magnitude larger than the value reported in literature and almost negligible for the anthracite layer.

Hence, a model has been developed that takes into account the main characteristics of (submerged) rapid filtration and that generally coincides with data obtained from drinking production sites: water quality parameters including alkalinity, temperature and pH, chemical speciation, homogeneous oxidation in the supernatant layer, heterogeneous oxidation kinetics and filter bed properties found in single and dual media filtration.

Acknowledgements

This research is financed by the Joint Research Programme of the Dutch Water Companies (BTO) and by research projects funded by the Dutch drinking water company Vitens N.V. through several BTO projects. Analysis of water quality parameters for the Holten and Velddriel case have been carried out by the Vitens laboratory (Vitens Solutions). Discussions with members of the project steering committee are highly appreciated (a.o. Simon Dost, WLN). We would like to thank Emile Cornelissen and Arslan Ahmad for reviewing the manuscript and Wolter Siegers (KWR) for performing the glovebox experiments with the filter material collected at Velddriel, Patrick Teunissen (Vitens), Martijn Tas (Vitens) and Jan van de Kamp (Vitens) for their cooperation and collection of the samples at production sites Holten and Velddriel, and Bas Wols (KWR) for assisting in the simulations with the nitrification model.

Literature

Aa, L. van der, Kors, L., Wind, A., Hofman, J., Rietveld, L., 2002. Nitrification in rapid sand filter: phosphate limitation at low temperatures. Water science and technology: water supply 2(1), 37–46.

Beek, C.G.E.M. van, Hiemstra, T., Hofs, B., Nederlof, M.M., Paassen, J.A.M. van, Reijnen, G.K., 2012a. Homogeneous, heterogeneous and biological oxidation of iron(II) in rapid sand filtration. J Water SRT — AQUA 61(1), 1–13.

Beek, C.G.E.M. van, Hiemstra, T., Hofs, B., Nederlof, M.M., Paassen, J.A.M. van, Reijnen, G.K., 2012b. Homogeneous, heterogeneous and biological oxidation of iron(II) in rapid sand filtration. J Water SRT — AQUA 61(1), 1–13.

Bruins, J., 2016. Improved manganese removal from groundwater.

Buamah, R., Petrusevski, B., Ridder, D. de, Wetering, T. van de, Shippers, J., 2009. Manganese removal in groundwater treatment: practice, problems and probable solutions. Water science and technology: water supply 9(1), 89–98.

Buamah, R., Petrusevski, B., Schippers, J., 2009. Oxidation of adsorbed ferrous iron: kinetics and influence of process conditions (400554-029; iron removal; oxidation).

Çakmakci, M., Kinaci, C., Bayramoglu, M., Yildirim, Y., 2010. A modeling approach for iron concentration in sand filtration effluent using adaptive neuro-fuzzy model. Expert Systems with Applications 37(2), 1369–1373.

Carlson, K.H., Knocke, W.R., Gertig, K.R., 1997. Optimizing treatment through Fe and Mn fractionation. Journal American Water Works Association 89(4), 162–171.

Council, E., 1998. Council directive 98/83 about water quality intended for human consumption. Official Journal of the European Communities L 330, 32–54.

Davies, S.H.R., Morgan, J.J., 1989. Manganese(II) oxidation kinetics on metal oxide surfaces. Journal of Colloid and Interface Science 129(1), 63–77.

Davison, W., Seed, G., 1983a. The kinetics of the oxidation of ferrous iron in synthetic and natural waters. Geochimica et Cosmochimica Acta 47(1), 67–79.

Davison, W., Seed, G., 1983b. The kinetics of the oxidation of ferrous iron in synthetic and natural waters. Geochimica et Cosmochimica Acta 47(1), 67–79.

Diem, D., Stumm, W., 1984. Is dissolved Mn(II) being oxidized by O2 in absence of Mn-bacteria or surface catalysts? Geochimica et Cosmochimica Acta 48(7), 1571–1573.

Drinkwaterbesluit, 2011. . Rijksoverheid.

Dzombak, D.A., Morel, F.M.M., 1990. Surface Complexation Modeling: Hydrous Ferric Oxide. Wiley Interscience.

Graveland, A., 1971. Verwijdering van mangaan uit grondwater.

Ives, K.J., 1970. Rapid filtration. Water Research 4(3), 201–223.

Jegatheesan, V., Vigneswaran, S., 2005. Deep bed filtration: mathematical models and observations. Critical reviews in environmental science and technology 35(6), 515–569.

Jez-Walkowiak, J., Dymaczewski, Z., Weber, L., others, 2015. Iron and manganese removal from groundwater by filtration through a chalcedonite bed. Journal of Water Supply: Research and Technology—AQUA 64(1), 19–34.

Kirby, C., Thomas, H., Southam, G., Donald, R., 1999. Relative contributions of abiotic and biological factors in Fe (II) oxidation in mine drainage. Applied Geochemistry 14(4), 511–530.

Liu, C., Zachara, J.M., Gorby, Y.A., Szecsody, J.E., Brown, C.F., 2001. Microbial reduction of Fe (III) and sorption/precipitation of Fe (II) on Shewanella putrefaciens strain CN32. Environmental science & technology 35(7), 1385–1393.

Michalakos, G.D., Nieva, J.M., Vayenas, D.V., Lyberatos, G., 1997. Removal of iron from potable water using a trickling filter. Water Research 31(5), 991–996.

Mouchet, P., 1992. From conventional to biological removal of iron and manganese in France. Journal of the American Water Works Association 84:4, 158–167.

Parkhurst, D.L., Appelo, C., 2013. Description of input and examples for PHREEQC version 3 A computer program for speciation, batch-reaction, one-dimensional transport, and inverse geochemical calculations. US Geological Survey Techniques and Methods, Book 6, Modeling Techniques.

Parkhurst, D.L., Appelo, C.A.., 1999. User's guide to PHREEQC (version 2)—A computer program for speciation, batch-reaction, one-dimensional transport, and inverse geochemical calculations. U.S. Department of the interior, Denver, Colorado, U.S.A.

Rentz, J.A., Kraiya, C., Luther, G.W., Emerson, D., 2007. Control of Ferrous Iron Oxidation within Circumneutral Microbial Iron Mats by Cellular Activity and Autocatalysis. Environmental Science & Technology 41:17, 6084–6089.

Schoonenberg Kegel, F., 2013. Optimization of the iron removal in rapid sand filters. Increase of the heterogenic iron removal by the reduction of the supernatant level, Bachelors thesis.

Schoonenberg Kegel, F., 2015. Removal of iron under anoxic conditions: removing iron by operating rapid sand filters in intermittent regeneration mode, Masters thesis.

Schwager, A., Boller, M., 1997. Transport phenomena in intermittent filters. Water Science and Technology 35(6), 13–20.
Sharma, S.K., 2001. Adsorptive iron removal from groundwater.
Sharma, S.K., Petrusevski, B., Schippers, J.C., 2005. Biological iron removal from groundwater: A review. Journal of Water Supply: Research and Technology - AQUA 54, 239–247.
Sommerfeld, E.O., 1999. Iron and manganese removal handbook. American Water Works Association.
Stumm, W., Lee, G.F., 1961. Oxygenation of Ferrous Iron. Industrial & Engineering Chemistry 53:2, 143–146.
Sung, W., Morgan, J.J., 1980. Kinetics and product of ferrous iron oxygenation in aqueous systems. Environmental Science & Technology 14:5, 561–568.
Tamura, H., Goto, K., Nagayama, M., 1976. The effect of ferric hydroxide on the oxygenation of ferrous ions in neutral solutions. Corrosion Science 16(4), 197–207.
Tamura, H., Kawamura, S., Hagayama, M., 1980. Acceleration of the oxidation of Fe2+ ions by Fe(III)-oxyhydroxides. Corrosion Science 20:8–9, 963–971.
Teunissen, K., 2007. Iron removal at groundwater pumping station Harderbroek.
Theis, T.L., Singer, P.C., 1974. Complexation of iron(II) by organic matter and its effect on iron(II) oxygenation. Environmental Science & Technology 8:8, 569–573.
Vet, W. de, Dinkla, I., Rietveld, L., Loosdrecht, M. van, 2011. Biological iron oxidation by Gallionella spp. in drinking water production under fully aerated conditions. Water research 45(17), 5389–5398.

Attachment I PHREEQC code blocks

Heterogeneous oxidation as explained in paragraph 2.3.2 is implemented by the following code in the PHREEQC database file and illustrated for the iron removal case. Firstly, iron ions are specified as two different species Fd and Ft, relating to Fe^{+2} and Fe_{+3} respectively.

Code excerpt from the PHREEQC-database file describing the rate of heterogeneous oxidation of iron(II) (in PHREEQC defined as Fd+2), comments are preceded by #.

```
RATES # (PHREEQC DAT-file)

Fd_ox_hfo # oxidation of adsorbed iron (heterogeneous oxidation)

-start
10  Fd     = MOL("Fd+2")
30  p_o2   = 10^(SI("O2(g)"))
35  Fd_ads = MOL("Hfo_sOFd+") + MOL("Hfo_wOFd+") + MOL("Hfo_wOHFd+2")
40  k_ox = PARM(1)
120 Fd_ads_ox = k_ox * Fd_ads * MOL("O2") * TIME # Tamura1976
190 if (Fd_ads_ox > (MOL("Hfo_wOHFd+2")+MOL("Hfo_wOFd+"))) then
       Fd_ads_ox = MOL("Hfo_wOHFd+2")+MOL("Hfo_wOFd+")
200 SAVE Fd_ads_ox
-end
```

Code excerpt from the main PHREEQC file that specifies the Freundlich rate constants related to iron(II):

```
SURFACE_SPECIES # (PHREEQC PHRQ-file)

Hfo_wOH + .225Fd+2 = Hfo_wOHFd+2
       -no_check
       -mole_balance Hfo_wOHFd+2
       log_k -2.126 # determined for middle layer Velddriel,
                    # 1/n = 0.225
<…> # other code blocks

SURFACE 1-20 # a single medium filter divided in 20 cells
       equil  solution 21
       Hfo_w  Ferrihydrite eq 1 5.33e4
```

Attachment II: Nitrification

Incorporation of nitrification in model

Nitrification is described as the conversion of ammonia to nitrite by nitroso-bacteria followed by the conversion of nitrite to nitrate by nitro-bacteria. Nitrification is represented by the reactions presented in Eq. 1 and 2 (van der Aa *et al.*, 2002):

$$2\,NH_4^+ + 3O_2 \xrightarrow{Nitroso-bacteria} 2NO_2^- + 2H_2O + 4H^+ \quad (1)$$

$$2NO_2^- + O_2 \xrightarrow{Nitro-bacteria} 2NO_3^- \quad (2)$$

Nitrification is included in the model by implementing Eq. 1 and 2. This model is set-up like many biological growth and consumption models: the specific growth rate of the micro-organism increases with available substrate and other rate-limiting compounds according to a saturation curve. In this model, the saturation curve is determined by half-saturation constants for phosphate, ammonium and oxygen and a specific maximum growth rate constant. Consumption of substrate is determined by the available biomass and a yield factor. A higher ratio of (maximal) growth rate versus biomass yield factor (μ/Y) means that more substrate (here: ammonium, oxygen or phosphate) is removed for accumulation of biomass. A maintenance rate constant determines the point at which bacteria do not grow exponentially but reaches equilibrium in biomass accumulation, death rate and energy needed for maintenance. The following equations were used:

$$\mu_S^{pot} = \frac{[S]}{K_S+[S]} \cdot \mu^{max} \quad (3)$$

$$\mu^{spec} = \min(\mu_{S_1}^{pot}, \mu_{S_2}^{pot}, \dots) \quad (4)$$

$$r_S = -\mu^{spec}\frac{[X]}{Y_S} \quad (5)$$

In which:

μ	=	growth rate	[1.s^{-1}]
[S]	=	concentration substrate	[g.m^{-3}]
K_s	=	Michaelis constant resp. affinity value for substrate S	[g.m^{-3}]
[X]	=	concentration bacteria	[g dw.m^{-3}]
r_s	=	volumic conversion rate substrate S	[g.s^{-1}.m^{-3}]
Y_s	=	yield on substrate S	[g dw.g^{-1}]
pot	=	potential	[-]
spec	=	specific	[-]
S	=	substrate	[-]
max	=	maximum	[-]

Further assumptions and model characteristics are listed below:

- The bacteria are assumed to be immobile and already present in biofilms that cover the filter media in the RSF. Hence convective transport of bacteria ? is neglected;
- The potential growth rate is determined by the limiting substrate, i.e. being ammonium, phosphate or oxygen. In case of complete nitrification the ammonium, respectively nitrite concentration is the limiting substrate for the Nitroso, respectively Nitrospira-bacteria;
- Temperature and pH dependence is incorporated, according to (van der Aa *et al.*, 2002)
- The influence of diffusion from the bulk liquid into the biofilm is not incorporated.

Model parameter values were collected and varied using two data sources (Van der Aa et al., 2002; STIMELA) as a basis. The values as reported in van der Aa et al. (2002) and STIMELA are shown in

- Table II - 1II - 1 and Table II - 2 for the species Nitrosomonas and Nitrospira, respectively.

- Although nitrification is responsible for part of oxygen depletion, for aerated filters oxygen is not limiting in the removal of iron and manganese in concentrations as found in raw ground waters.
- The values used for various simulations are shown in Table II - 3.

TABLE II - 1: GROWTH RATE, MAINTENANCE RATE CONSTANTS AND BIOMASS YIELD VALUES OF THE SPECIES NITROSOMONAS

Nitrosomonas	**Maximal specific growth rate**	**Maintenance rate constant**	**Biomass yield factor**	**Maximal consumption ratio**
PHREEQC tag	*muMax15_Ns*	*b_Ns*	*Y_Ns*	*muMax15_Ns/Y*
unit	*1/s*	*1/s*	*(g d.s./m³)/(mg NH_4-N/L)*	*(mg NH_4-N/L)/ (s g d.s./m³)*
Most likely value[1]	$3.70 \cdot 10^{-5}$	$1.00 \cdot 10^{-6}$	0.12	$3.08 \cdot 10^{-4}$
Min. value[1]	$1.70 \cdot 10^{-5}$	$4.60 \cdot 10^{-7}$	0.04	$4.25 \cdot 10^{-4}$
Max. value[1]	$7.90 \cdot 10^{-5}$	$4.00 \cdot 10^{-6}$	0.17	$4.65 \cdot 10^{-4}$
Value in STIMELA	$5.00 \cdot 10^{-6}$	$2.00 \cdot 10^{-7}$	0.15	$3.33 \cdot 10^{-5}$

[1] van der Aa *et al.* (2002)

TABLE II - 2: GROWTH RATE, MAINTENANCE RATE CONSTANTS AND BIOMASS YIELD VALUES OF THE SPECIES NITROSPIRA

Nitrospira	**Maximal specific growth rate**	**Maintenance rate constant**	**Biomass yield factor**	**Maximal consumption ratio**
PHREEQC tag	muMax15_Ns	b_Ns	Y_Ns	muMax15_Ns/Y
unit	1/s	1/s	(g d.s./m³)/(mg NH_4-N/L)	(mg NH_4-N/L)/ (s g d.s./m³)
Mean value[1]	$1.00 \cdot 10^{-6}$	$3.00 \cdot 10^{-6}$	0.05	$6.00 \cdot 10^{-5}$
Min. value[1]	$4.60 \cdot 10^{-7}$	$7.30 \cdot 10^{-7}$	0.04	$1.83 \cdot 10^{-5}$
Max. value[1]	$4.00 \cdot 10^{-6}$	$4.80 \cdot 10^{-6}$	0.06	$8.00 \cdot 10^{-5}$
Value in STIMELA	$2.00 \cdot 10^{-7}$	$9.00 \cdot 10^{-6}$	$6.00 \cdot 10^{-2}$	$1.50 \cdot 10^{-4}$

[1] van der Aa *et al.* (2002)

TABLE II - 3: OVERVIEW OF NITRIFICATION MODEL PARAMETER CONSTANTS

	Nitrosomonas					Nitrospira			
PHREEQC tag	Maximal specific growth rate muMax15_Ns	Maintenance rate constant b_Ns	Biomass yield factor Y_Ns	Monod constant for NH_4 KsNH4_Ns_0	Initial condition	Maximal specific growth rate b_Nb	Maintenance rate constant muMax15_Nb	Biomass yield factor Y_Nb	pH correction
unit	1/s	1/s	(g d.s./m3)/ (mg NH4-N/L)	mg/L	g d.s./m3	1/s	1/s	(g d.s./m3)/(mg NH4-N/L)	
Simulation no. and figure									
1	3.70E-05	1.00E-06	0.12	0.405	0.2	1.00E-06	3.00E-06	0.05	True
2	5.00E-06	2.00E-07	0.15	0.405	0.2	2.00E-07	9.00E-06	6.00E-02	True
3	3.70E-05	4.00E-06	0.12	0.405	0.2	1.00E-06	3.00E-06	0.05	True
4	3.70E-05	2.00E-06	0.12	0.405	0.2	1.00E-06	3.00E-06	0.05	True
5	1.70E-05	1.00E-06	0.12	0.405	0.2	1.00E-06	3.00E-06	0.05	True
6	7.90E-05	1.00E-06	0.12	0.405	0.2	1.00E-06	3.00E-06	0.05	True
7	3.00E-05	1.00E-06	0.12	0.405	0.2	1.00E-06	3.00E-06	0.05	True
8	3.70E-05	1.25E-06	0.12	0.405	0.2	1.00E-06	3.00E-06	0.05	True
9	2.60E-05	1.00E-06	0.12	0.2	0.02	1.00E-06	3.00E-06	0.05	True
10	2.05E-05	1.00E-06	0.12	0.1	0.02	1.00E-06	3.00E-06	0.05	True
11	3.70E-05	1.00E-06	0.12	0.405	0.02	1.00E-06	3.00E-06	0.05	True
12	3.70E-05	1.00E-06	0.1	0.405	0.02	1.00E-06	3.00E-06	0.05	True
13	1.00E-05	1.00E-06	0.12	0.01	0.02	1.00E-06	3.00E-06	0.05	True
14	3.70E-05	1.00E-06	0.012	0.405	0.02	1.00E-06	3.00E-06	0.05	True
17	1.00E-05	2.00E-07	0.012	0.405	0.02	1.00E-06	3.00E-06	0.05	True
18	2.00E-05	2.00E-07	0.012	0.405	0.02	1.00E-06	3.00E-06	0.05	True
19	8.00E-06	2.00E-07	0.012	0.405	0.02	1.00E-06	3.00E-06	0.05	True
20	5.00E-06	2.00E-07	0.012	0.405	0.02	1.00E-06	3.00E-06	0.05	True
21	6.00E-06	2.00E-07	0.012	0.405	0.02	1.00E-06	3.00E-06	0.05	False (0.14)

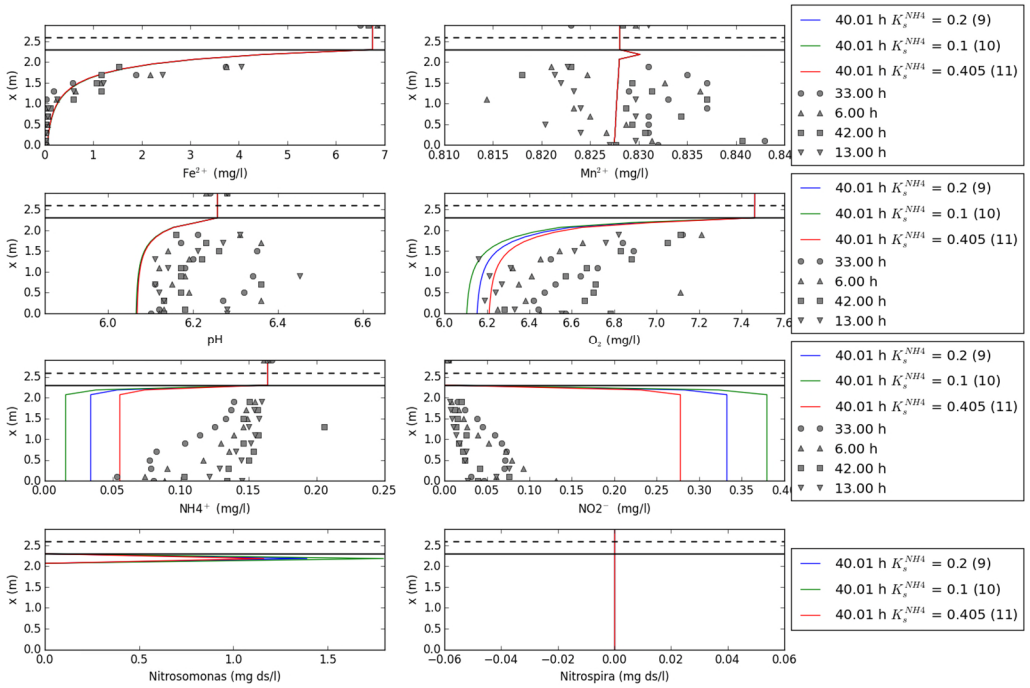

FIGURE II - 1 – VARIATION IN MONOD CONSTANT FOR NH_4

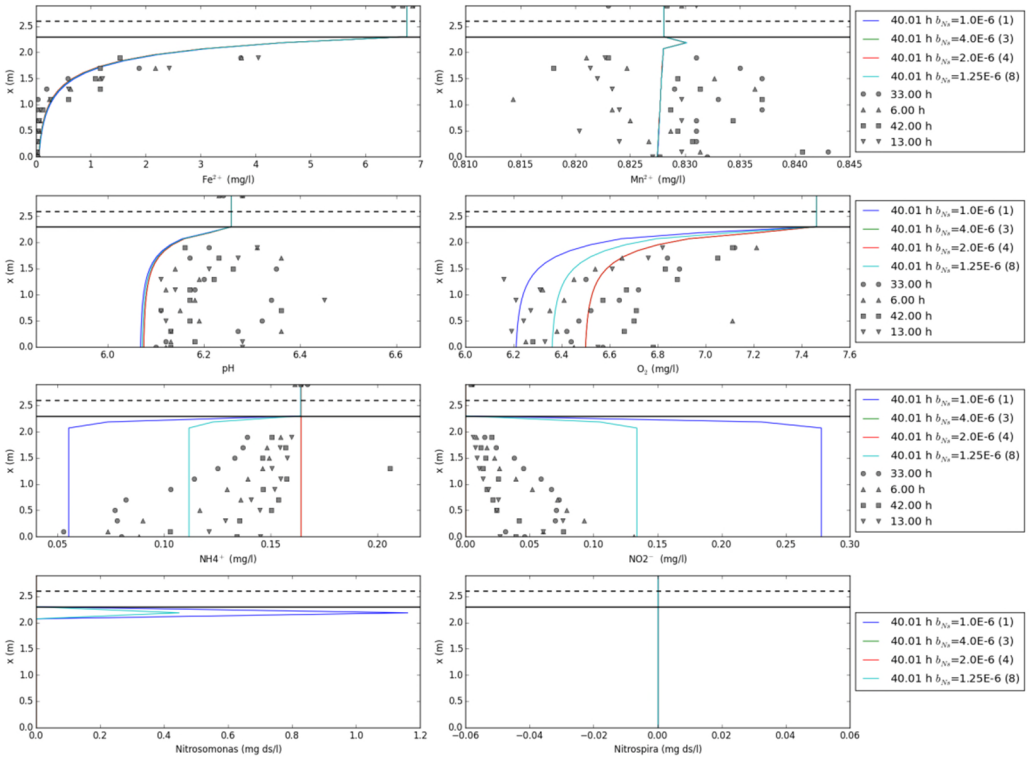

FIGURE II-2 – VARIATION IN MAINTENANCE RATE CONSTANT (B_{NS})

Results

Figure II-1 and II-2 show that Nitrosomonas mainly survives in the top layer of the sand filter. However, this effect is not supported by the results from the qPCR analysis performed on the filter material from Velddriel.

To determine the quantity of ammonia oxidizing bacteria (AOB) and archae (AOA), water and sand samples were taken on four dates: 14 November 2014, 11 December 2014, 6 March 2015, and 9 April 2015. As an example, the results of the sampling campaign on 6 March are presented below in Figure II-3 (results of the other sampling dates are presented in BTOs report "Research pilot and modelling of filtration at Velddriel: iron, manganese and ammonium removal" BTO 2016.204(s)). It has to be noted that the efficiency of the DNA extraction of the anthracite sample was too low to, thus the uncertainty (error) is rather large for this sample and results can only be interpreted indicatively.

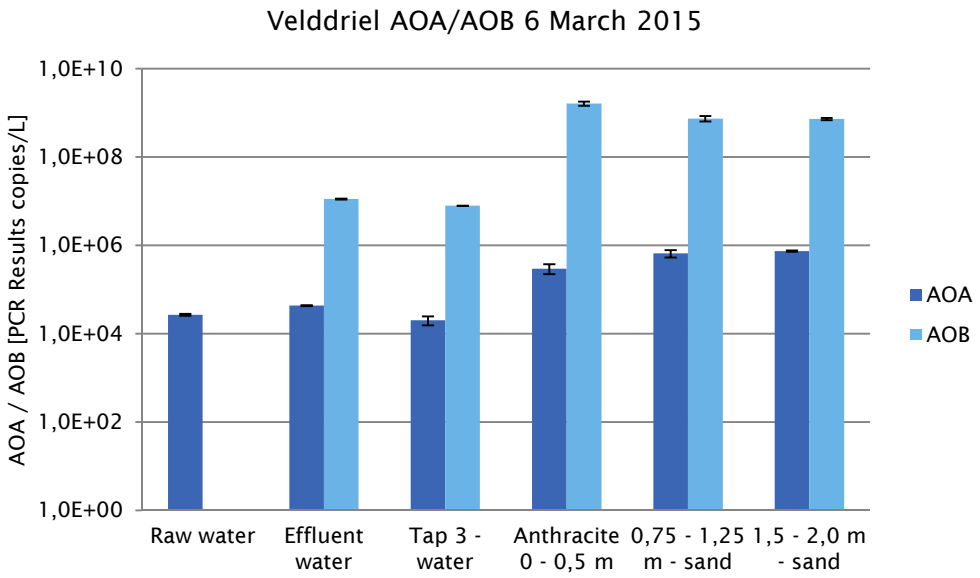

FIGURE II-0-1: QUANTITY AMMONIA OXIDIZING ARCHAE (AOA) AND BACTERIA (AOB) IN WATER AND SAND SAMPLES ON 6 MARCH 2015. NB. RAW WATER SAMPLE WAS NOT ANALYSED FOR AOB.

From Figure 3-3 it seems that the quantity of AOB and AOA in sand samples is in general higher than in water samples. This corresponds to earlier findings of Kramer et al. (2012) who concluded that ATP concentrations were higher and showed less variability in the soil phase compared to the water phase.

The AOA and AOB seems to be evenly distributed over the filter height, while it was expected that most AOB and AOA would be present in the initial phase of the filter (first few centimetres) van der Aa et al. (2002). This could be explained by the relatively low running time of the filter (only 3 months). It is possible that the distribution of AOA and AOB will change as a result of filter running time.

In addition, the quantity of AOA seems to be generally lower than the quantity of AOB (approximately a factor 10^3 for water samples and a factor 10^4 for sand samples).

Although some trends are observed in the results of the AOA and AOB analysis, data obtained in this study is limited to a small amount of samples. More data is required to confirm and generalize the above observations.

Literature

Aa, L. van der, Kors, L., Wind, A., Hofman, J. A. M. H., & Rietveld, L. (2002). Nitrification in rapid sand filter: phosphate limitation at low temperatures. *Water Science and Technology: Water and Supply*, *2*(1), 37–46. Retrieved from http://ws.iwaponline.com/content/2/1/37

Kramer, F. (2012). *Removal of Organic Micro Pollutants in Batch Experiments Mimicking Riverbank Filtration*. TU Delft, Delft University of Technology.

Rietveld, L. C., Helm, A. van der, Schagen, K. van, Aa, R. van der, & Dijk, H. van. (2008). Integrated simulation of drinking water treatment. *Journal of Water Supply: Research and Technology - AQUA*, *57*(3), 133–141. doi:10.2166/aqua.2008.098

Attachment III Simulation and measured data from production plants

WPB De Punt

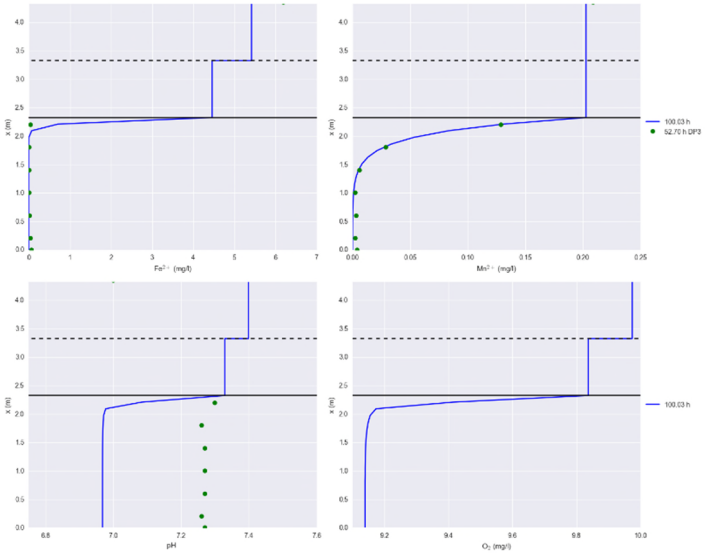

FIGURE 0-2: BED HEIGHT PROFILE, MEASURED FROM THE BOTTOM OF THE RSF. FROM LEFT TO RIGHT, AND FROM TOP TO BOTTOM: IRON(II), MANGANESE (II), PH AND OXYGEN CONCENTRATION. MEASUREMENTS (DOTS), SIMULATION RESULTS (BLUE LINE), SUPERNATANT LEVEL (BLACK LINE) AND TOP OF THE FILTER BED (BLACK DASHED LINE).

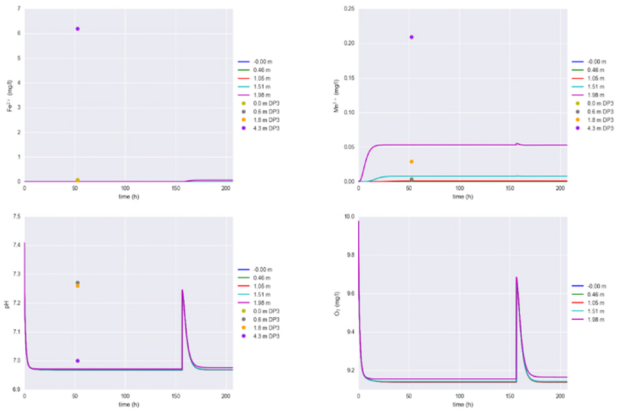

FIGURE 0-3: EVOLUTION OF (FROM LEFT TO RIGHT): IRON(II), MANGANESE(II), BELOW: PH AND OXYGEN CONCENTRATION

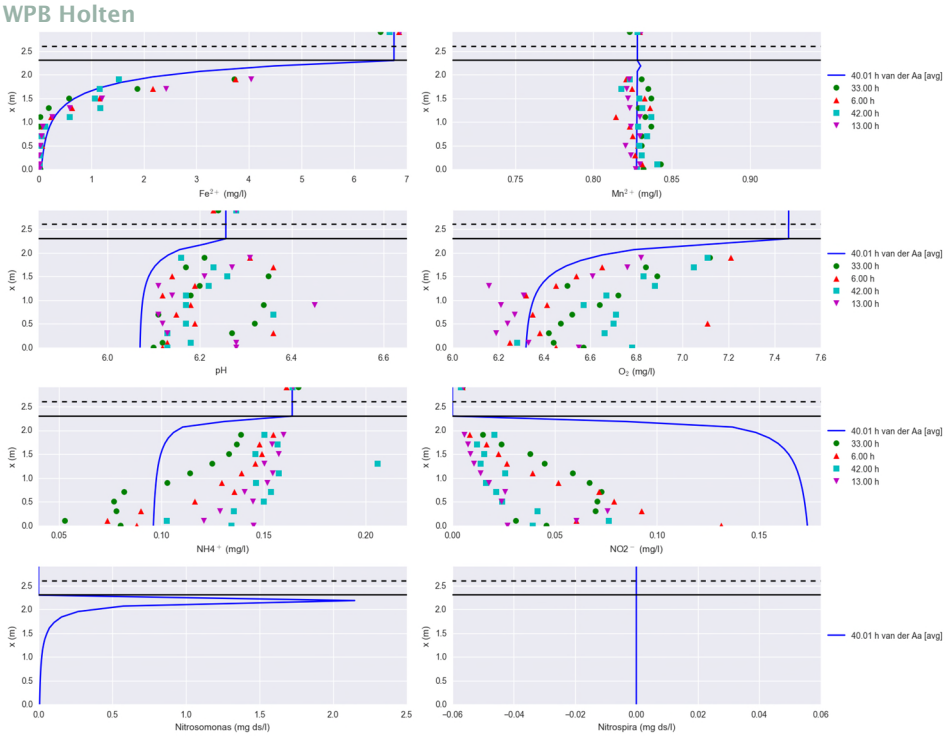

FIGURE 0-4: BED HEIGHT PROFILE, MEASURED FROM THE BOTTOM OF THE RSF. FROM LEFT TO RIGHT, AND FROM TOP TO BOTTOM: IRON(II), MANGANESE (II), PH AND OXYGEN CONCENTRATION. MEASUREMENTS (DOTS), SIMULATION RESULTS (BLUE LINE), SUPERNATANT LEVEL (BLACK DASHED LINE) AND TOP OF THE FILTER BED (BLACK LINE).

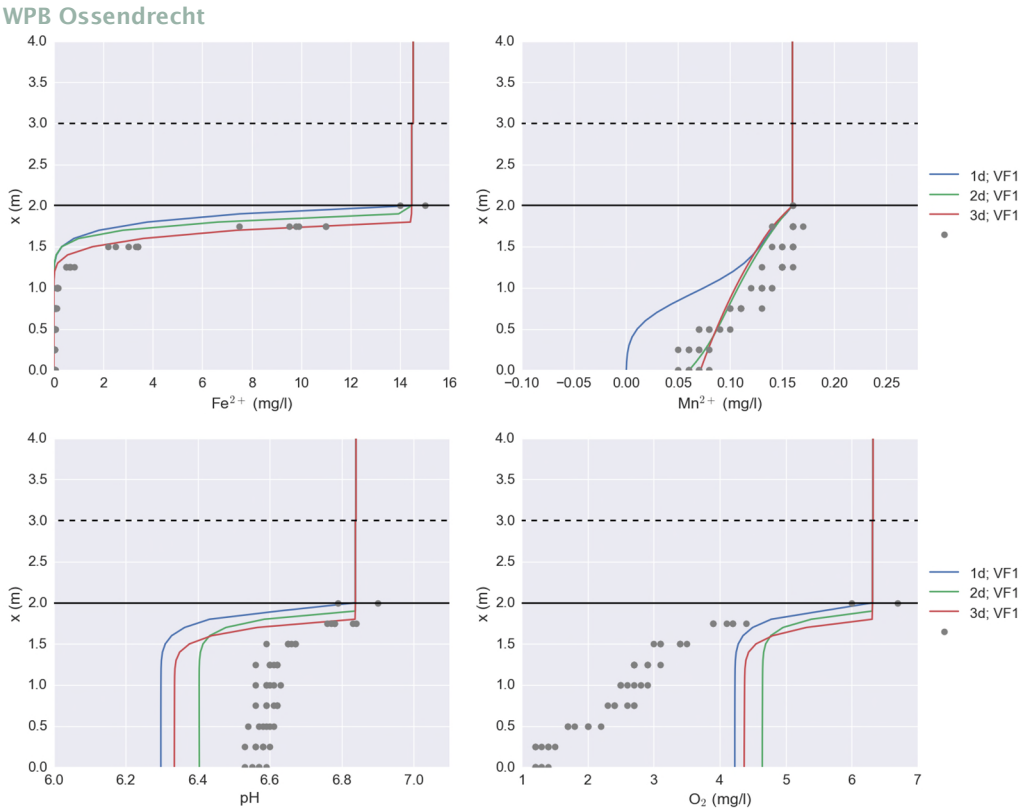

FIGURE 0-5: BED HEIGHT PROFILE, MEASURED FROM THE BOTTOM OF THE RSF AT OSSENDRECHT. FROM LEFT TO RIGHT, AND FROM TOP TO BOTTOM: IRON(II), MANGANESE (II), PH AND OXYGEN CONCENTRATION. MEASUREMENTS (DOTS), SIMULATION RESULTS (BLUE (1 DAY), GREEN (2 DAYS OF FILTRATION TIME) AND RED LINE (3 DAYS OF FILTRATION TIME)), SUPERNATANT LEVEL (BLACK DASHED LINE) AND TOP OF THE FILTER BED (BLACK LINE).

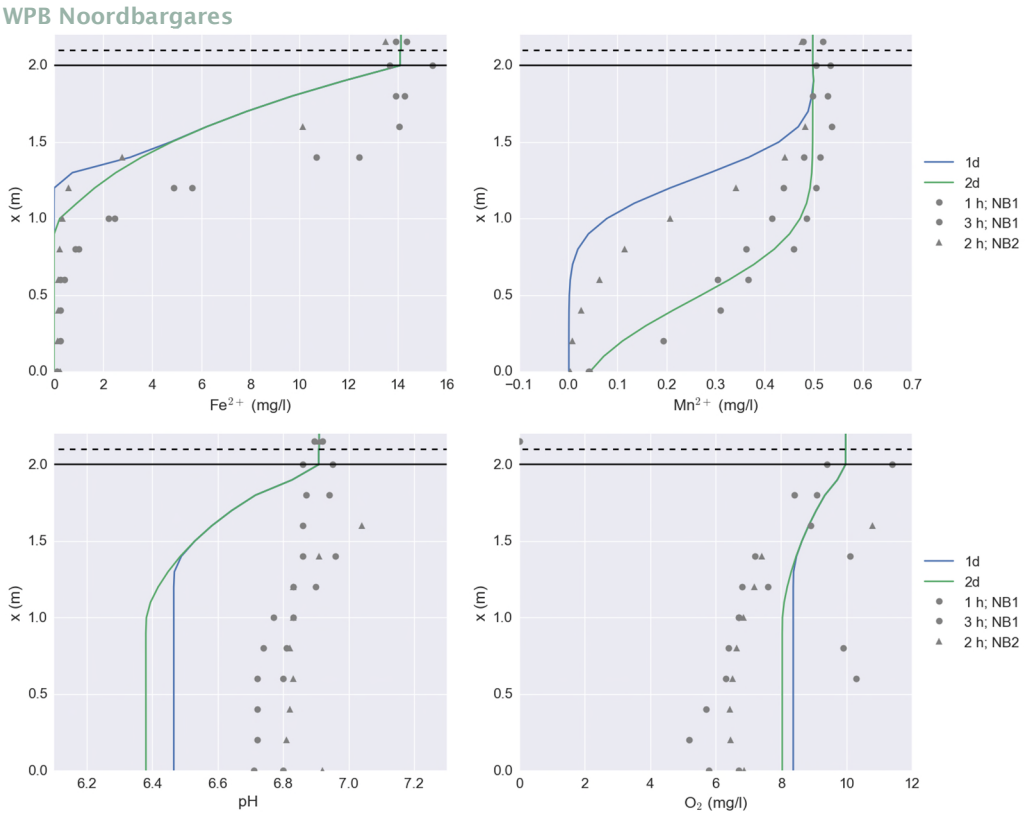

FIGURE 0-6: BED HEIGHT PROFILE, MEASURED FROM THE BOTTOM OF THE RSF AT NOORDBARGARES. FROM LEFT TO RIGHT, AND FROM TOP TO BOTTOM: IRON(II), MANGANESE (II), PH AND OXYGEN CONCENTRATION. MEASUREMENTS (GREY MARKERS), SIMULATION RESULTS (BLUE (1 DAY OF FILTRATION TIME), GREEN (2 DAYS OF FILTRATION TIME)), SUPERNATANT LEVEL (BLACK DASHED LINE) AND TOP OF THE FILTER BED (BLACK LINE).

MANGANESE OXIDATION RATE CONSTANT OF $2.4 \cdot 10^{-4}$ s^{-1} IS ASSUMED.

Attachment IV Simulated bed profiles using the determined Freundlich constants at WPB Velddriel

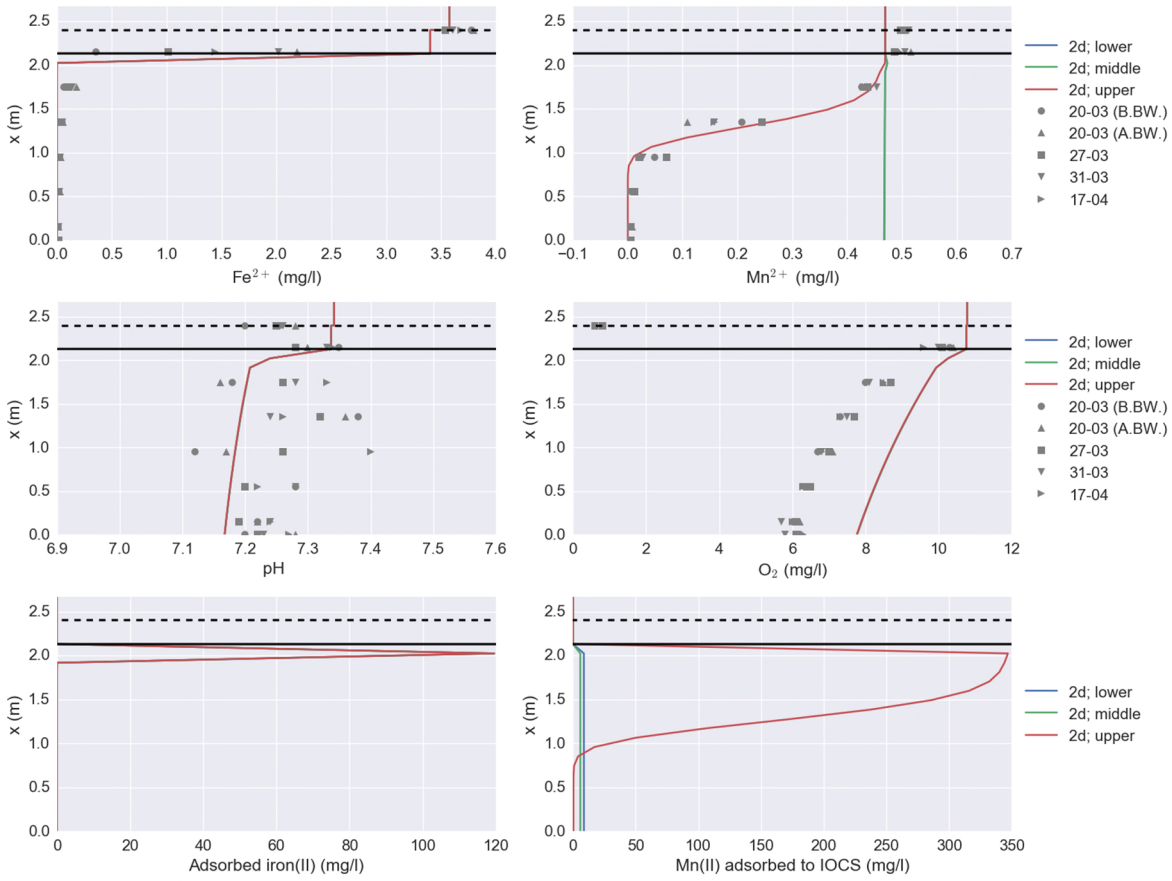

FIGURE 0-7: SIMULATION WITH DIFFERENT FREUNDLICH CONSTANTS, CORRESPONDING TO THE SAMPLES TAKEN AT THE UPPER LAYER (RED), MIDDLE LAYER (GREEN) AND LOWER LAYER (BLUE) OF THE FILTER BED.

Attachment V Effect of the heterogeneous oxidation rate on manganese removal

Simulation case for production site Velddriel

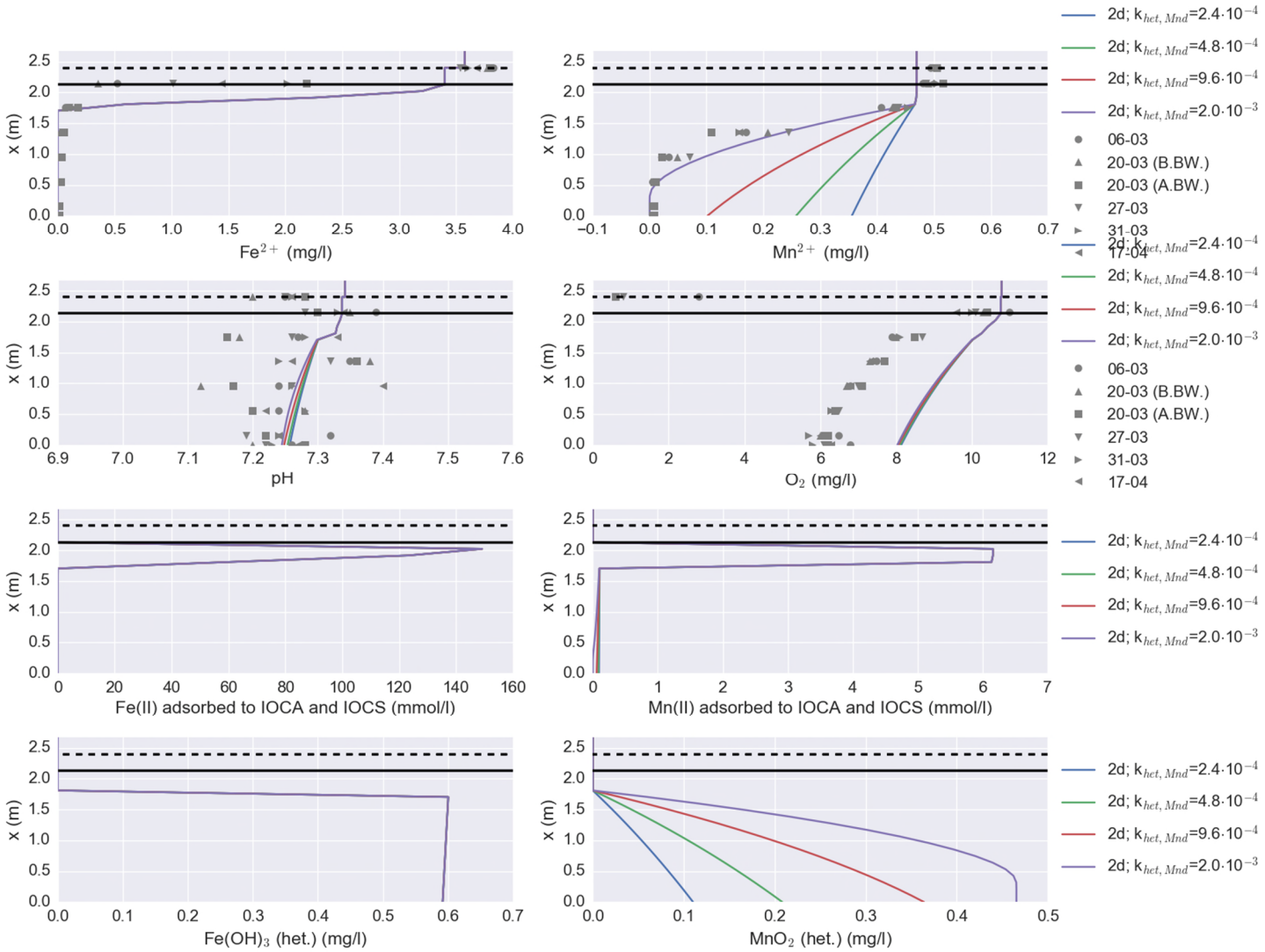

FIGURE 0-8: EFFECT OF HETEROGENEOUS MANGANESE OXIDATION RATE CONSTANT ON CONCENTRATION PROFILES (X AXIS) OVER THE FILTER BED (Y AXIS). UPPER PANEL: IRON(II) AND MANGANESE(II)

CONCENTRATIONS, 2ND ROW: PH AND OXYGEN CONCENTRAION, 3RD ROW: IRON(II) AND MANGANESE(II) ADSORBED TO IRON OXIDIZED COATED ANTHRACITE (IOCA) AND – SAND (IOCS), 4TH ROW: FORMED IRON AND MANGANESE OXIDES.

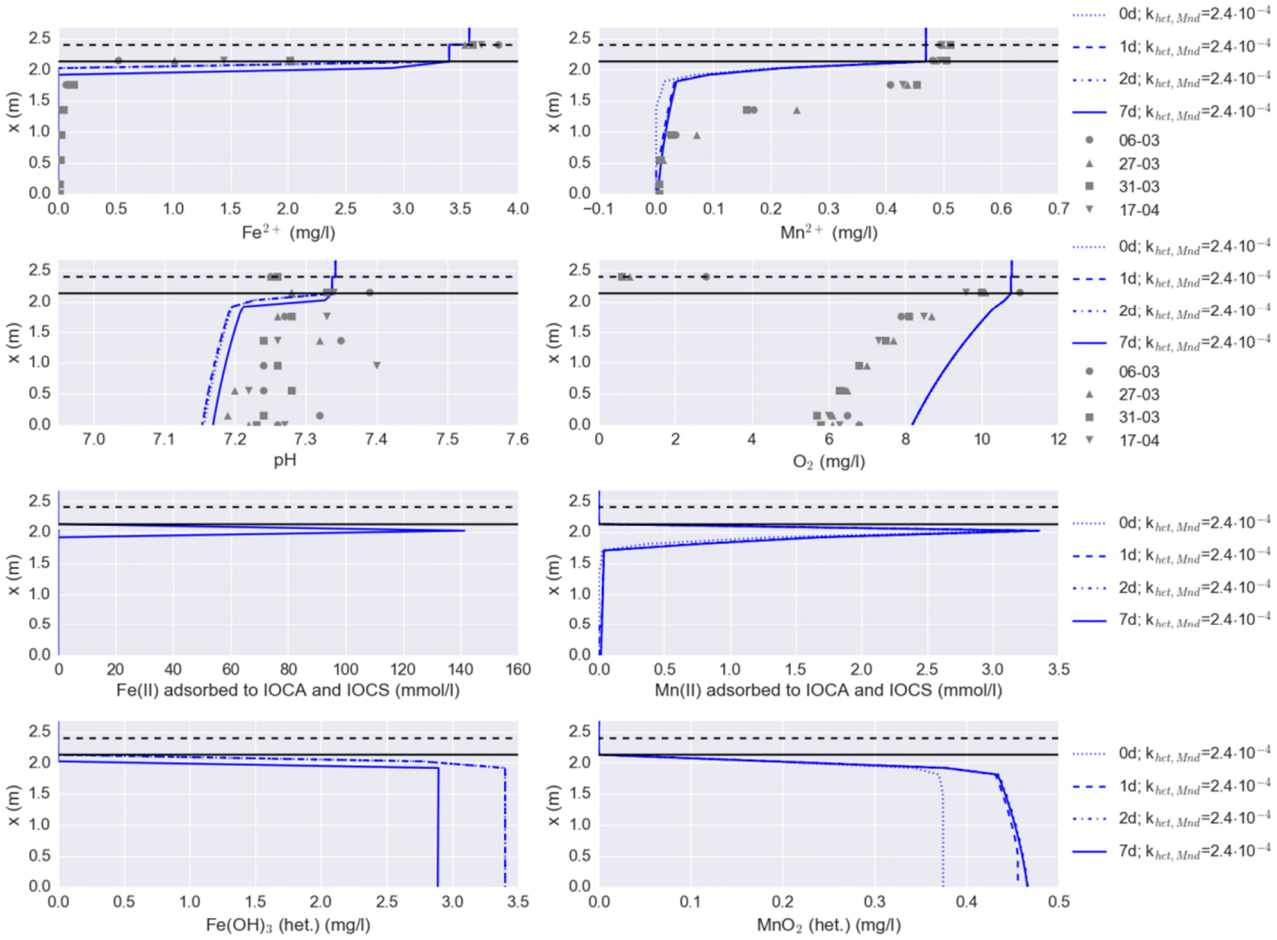

FIGURE 0-9: SIMULATED RSF (BLUE LINES) WITH $k_{HET,MND}$ = $2.4 \cdot 10^{-4}$ s^{-1} (ADOPTED FROM DAVIES ET AL., 1988) FOR BOTH FILTER LAYERS AND MEASURED (GREY MARKERS) IRON(II) AND MANGANESE (II) CONCENTRATIONS OVER BED HEIGHT (1ST ROW), PH AND OXYGEN CONCENTRATION (2ND ROW), AMOUNT OF ADSORBED IONS (3RD ROW) AND FORMED OXIDES (4TH ROW) SIMULATED AT DIFFERENT FILTER RUN TIMES IN DAY UNITS (FROM 12H TO 7 DAYS).